The Canadian Mineralogist
Vol. 35, pp. 367-396 (1997)

DIVERSE PRIMITIVE MAGMAS IN THE CASCADE ARC, NORTHERN OREGON AND SOUTHERN WASHINGTON

RICHARD M. CONREY[1]

Department of Geology, Washington State University, Pullman, Washington 99164, U.S.A.

DAVID R. SHERROD[2]

U.S. Geological Survey, Hawaiian Volcano Observatory, P.O. Box 51, Hawaii National Park, Hawaii 96718, U.S.A.

PETER R. HOOPER[3]

Department of Geology, Washington State University, Pullman, Washington 99164, U.S.A.

DONALD A. SWANSON[4]

U.S. Geological Survey, Hawaiian Volcano Observatory, P.O. Box 51, Hawaii National Park, Hawaii 96718, U.S.A.

ABSTRACT

Bulk-rock major- and trace-element composition, petrography and mineral compositions are presented for a diverse suite of 22 primitive mafic lavas in the Cascade Range of northern Oregon and southern Washington. With the exception of an early Western Cascade basalt, all the rocks are younger than 7 Ma. Intensive parameters [$f(H_2O)$, $f(O_2)$, T, P] for the magmas have been inferred mostly from equilibrium olivine–liquid and plagioclase–liquid relations. Nearly anhydrous, MORB-like, low-K tholeiite was probably derived from relatively high degrees of decompression-induced melting of shallow, depleted, relatively unmetasomatized lithospheric mantle during intra-arc rifting. The degree of partial melting decreases northward along the arc, whereas the depth of average melt generation increases. OIB-like basalt represents deeper, wetter, smaller-degree melts of more enriched asthenospheric mantle, unaffected by subduction. Olivine analcimite resembles the silicate melt considered responsible for within-plate mantle metasomatism. Post-7-Ma subduction-related basalt was derived by low degrees of partial melting of subduction–metasomatized garnet lherzolite, similar to OIB-like basalt source-mantle before modification. The spectrum of subduction-related basalt from cooler and wetter (and slightly more oxidized) absarokite to progressively hotter and drier high-K calc-alkaline basalt and calc-alkaline basalt seems to be due to varying degrees of metasomatism of the deep mantle wedge by relatively cool, wet, *LILE*-rich absarokitic magmas coming from near the subducted slab. Early Western Cascade basalt is more typically arc-like in its composition and mineralogy, and was probably generated under H_2O-rich conditions when more vigorous subduction prevailed. Depleted basaltic andesite may have been generated by low degrees of partial melting of residual harzburgite, possibly formed during the generation of early Western Cascade basalt.

Keywords: arc, basalt, primitive, absarokite, tholeiite, Cascade, intensive parameters, trace elements, intra-arc rifting, rift, Oregon, Washington.

SOMMAIRE

Nous présentons des données chimiques (éléments majeurs et traces), descriptions pétrographiques et caractérisations minéralogiques d'une suite d'échantillons divers provenant de 22 coulées de lave primitive dans la chaîne des Cascades, dans la partie nord de l'Oregon et la partie sud du Washington. A l'exception d'un basalte précoce dans le secteur ouest de la chaîne, toutes ces roches sont plus jeunes que 7 millions d'années. Les paramètres intensifs des magmas [$f(H_2O)$, $f(O_2)$, T, P] ont été évalués à partir des modèles d'équilibre impliquant olivine–liquide et plagioclase–liquide. Les magmas tholéiitiques à faible teneur en K, relativement anhydres et semblables aux magmas basaltiques des croûtes médio-océaniques, ont probablement été dérivés par fusion partielle à un taux relativement élevé, accompagnant la décompression d'un manteau lithosphérique relativement non métasomatisé pendant un épisode de rift intra-arc. Le degré de fusion partielle semble avoir diminué vers le nord le

E-mail addresses: [1] conrey@mail.wsu.edu, [2] dsherrod@liko.wr.usgs.gov, [3] prhooper@mail.wsu.edu, [4] donswan@liko.wr.usgs.gov.

long de l'arc, tandis que la profondeur du foyer de fusion partielle augmentait. Les basaltes semblables à ceux des îles océaniques représentent des volumes de magma d'origine plus profonde, plus riches en phase aqueuse, et issus par fusion partielle plus restreinte d'un manteau asthénosphérique plus fertile, mais non affecté par la subduction. L'analcimite à olivine représenterait la sorte de magma auquel on attribue la métasomatose du manteau dans les régions intra-plaques. Les basaltes liés à la subduction et plus jeunes que 7 millions d'années ont été dérivés par fusion partielle restreinte d'une lherzolite à grenat semblable au manteau sous les îles océaniques, mais modifié par métasomatose dans le milieu de subduction. Le spectre de laves basaltiques liées à la subduction, partant de magmas à caractère absarokitique, à température relativement faible, plus fortement oxydés et enrichis en H_2O, jusqu'aux magmas calco-alcalins enrichis ou non en K, à température plus élevée et plus secs, semble dû à un taux variable de métasomatose du socle mantellique par dessus la zone de subduction en réponse à des venues de magmas absarokitiques relativement fertiles dérivés de la zone proximale de la plaque en subduction. Le basalte précoce du secteur ouest de la chaîne des Cascades ressemble davantage à un produit typique d'un d'arc dans sa composition et sa minéralogie, et aurait été formé dans un milieu plus riche en H_2O lorsque la subduction y était plus vigoureuse. Les andésites basaltiques stériles pourraient bien avoir pris naissance suite à une fusion partielle à degré restreint d'une harzburgite résiduelle, peut-être au cours de la formation du basalte précoce du secteur ouest de la chaîne des Cascades.

(Traduit par la Rédaction)

Mots-clés: arc, basalte, primitif, absarokite, tholéiite, Cascades, paramètres intensifs, rift intra-arc, rift, Oregon, Washington.

INTRODUCTION

Primitive magmas in arcs are of interest because they contain the most information about source regions in the mantle and melting processes beneath arcs. Primitive magmas are least affected by fractionation and assimilation, and the presence of diverse primitive magmas implies corresponding diversity in mantle sources and melting processes. It is impossible to relate different, equally primitive magmas to one another by shallow-level fractionation and assimilation; the magmas must be derived from different sources or melting of similar sources under different conditions. Here we attempt to establish the intensive parameters and origins of diverse primitive Cascade arc magmas on the basis of their petrological features. The intensive parameters are then used to constrain petrogenetic models of the Cascade subduction zone. We report bulk-rock and phenocryst compositions of 22 primitive mafic lavas, derived from our basalt database (approximately 500 analyses) from northern Oregon and southern Washington. Earlier reports on mafic lavas in the Cascade arc have established the wide variety of rock types present, including low-K tholeiite, calc-alkaline basalt, primitive basaltic andesite, and shoshonite (Hughes & Taylor 1986, Bacon 1990, Hughes 1990, Leeman *et al.* 1990, Donnelly-Nolan *et al.* 1991, Baker *et al.* 1991, 1994). The mantle beneath the Cascade arc is considered to contain depleted mid-ocean ridge basalt (MORB) and ocean island basalt (OIB) source components, as well as subduction-metasomatized parcels. Mantle similar to OIB-source mantle seems to be more prevalent northward (*cf.* Bacon 1990, Leeman *et al.* 1990). Such diversity may be the rule in continental margin arcs, as a variety of primitive mafic lavas also are found in western Mexico (Luhr *et al.* 1989, Luhr 1996).

The origin of arc magmas is incompletely understood, although consensus is growing that contributions from both the subducted slab and mantle wedge are important (Kay 1984, Arculus & Powell 1986, McCulloch & Gamble 1991, Pearce & Parkinson 1993, Plank & Langmuir 1993, Woodhead *et al.* 1993, Stolper & Newman 1994, Pearce *et al.* 1995). The high-field-strength (*HFSE*) elements Nb, Ta, Zr, Hf, and Ti in the mantle wedge seem to be relatively unaffected by the subduction process, and faithfully record melting events in the wedge and backarc. Many other incompatible elements in the wedge, especially large-ion lithophile elements (*LILE*), are controlled to varying degrees by the subduction process.

Many details of that process are still uncertain. It is unknown if transport of incompatible elements from slab to wedge takes place *via* fluids or melts or both, but experimental and other evidence suggests that either mechanism results in creation of hydrous metasomatic phases, especially phlogopite, in the mantle wedge (Sekine & Wyllie 1982, Schneider & Eggler 1986, Tatsumi 1989, Sudo & Tatsumi 1990, McInnes & Cameron 1994). Reaction between an ascending hydrous melt and wedge peridotite may result in substantial modification of the melt's composition (Kelemen *et al.* 1993).

The melting relations of hydrous peridotite (*i.e.*, containing amphibole or phlogopite or both) are poorly known (Tatsumi & Koyaguchi 1989, Thibault *et al.* 1992), compared to the thorough knowledge of dry melting of spinel or plagioclase peridotite (Jaques & Green 1980, Falloon *et al.* 1988, Kinzler & Grove 1992, 1993, Langmuir *et al.* 1992, Hirose & Kushiro 1993). It is possible to infer the type of source, and depth and relative degree of partial melting of a number of Cascade primitive magmas, especially the drier ones. However, until the melting relations of wet peridotite are understood, it will not be possible to fully interpret the origin and evolution of water-rich magmas.

GEOLOGICAL SETTING

The Cascade arc has been continuously active since about 40 Ma (Lux 1982, Phillips *et al.* 1986, Verplanck

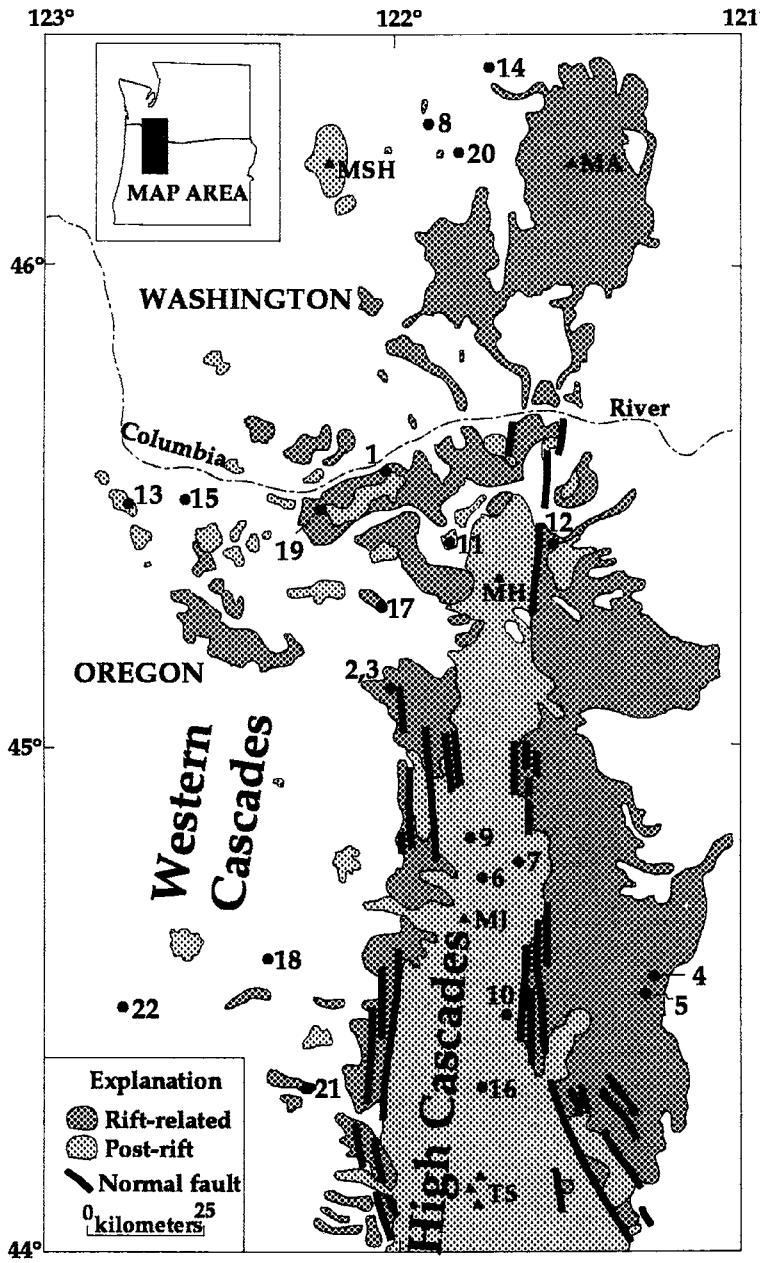

FIG. 1. Generalized geological map of the Cascade Range in northern Oregon and southern Washington, and location of samples analyzed for this paper. Locations of major composite stratocones (MSH: Mt. St. Helens, MA: Mt. Adams, MH: Mt. Hood, MJ: Mt. Jefferson, TS: Three Sisters) shown for reference. Rift-related rocks are ≤7.5 Ma south of MJ and progressively younger northward; all rift-related rocks in Washington are of Quaternary age. Post-rift rocks partly fill structural depressions formed during rifting or are late Quaternary in age (*e.g.*, MSH).

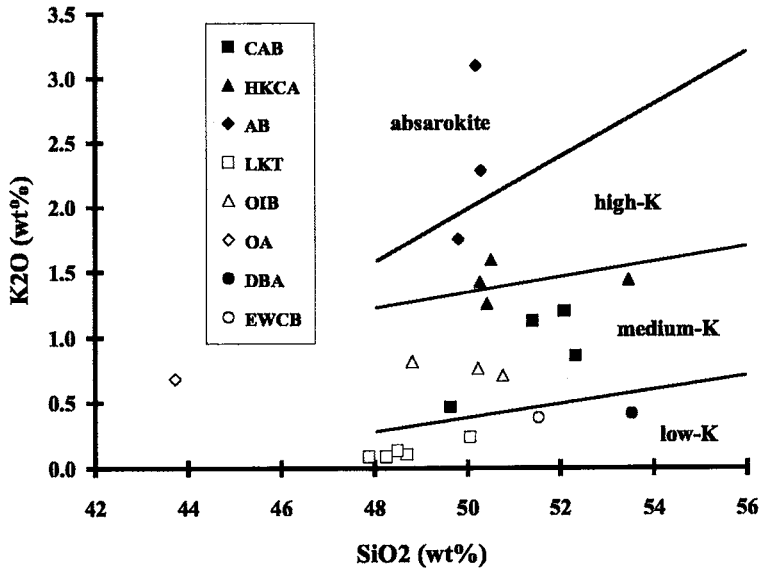

FIG. 2. Weight% K_2O *versus* SiO_2 for the primitive mafic lavas characterized in this paper. Note that the terminology used here does not exactly correspond to the designated fields shown (Peccerillo & Taylor 1976). LKT: low-K tholeiite, OIB: OIB-like basalt, OA: olivine analcimite, CAB: calc-alkaline basalt, HKCA: high-K calc-alkaline basalt, AB: absarokite, EWCB: early Western Cascade basalt, DBA: depleted basaltic andesite.

& Duncan 1987). The early history of the arc is relatively unstudied, especially in northern Oregon, where Miocene strata bury most older rocks, but it is probable that the early arc, until 17–15 Ma, was more active than later (Wells *et al.* 1984, Verplanck & Duncan 1987, Priest 1990). Eruption rates may have declined dramatically by about 17 Ma, along with a declining rate of convergence. Early Cascade arc rocks are more typically "arc-like" in that highly plagioclase-phyric mafic rocks with high levels of Al (19–20 wt% Al_2O_3) are widespread, and augite phenocrysts are common along with olivine in mafic lavas (Peck *et al.* 1964, Lux 1981, Verplanck 1985, Ritchie 1987). Anorthite (An_{90}) phenocrysts are present in some early arc lavas (Ritchie 1987).

The younger, post-17 Ma arc is notable for the development of a propagating intra-arc rift starting in central Oregon at about 7–8 Ma (Smith *et al.* 1987, Conrey *et al.* 1994, Conrey & Sherrod, unpubl. data). Rifting was associated with eruption of a wide compositional spectrum of lavas and ash-flow tuffs, including substantial amounts of low-K tholeiite. In most areas, substantial volumes of mafic lavas were erupted for about 2 million years, followed by foundering of the arc in a graben or half-graben. Those mafic rocks are termed "syn-rift" in this report. Post-faulting ("post-rift" in this report) eruptions largely bury the main axis of older syn-rift volcanism, hence syn-rift lavas are preserved on both flanks of the modern arc (Fig. 1). Rifting was time-transgressive and structurally discontinuous (Fig. 1) in northern Oregon: the rift propagated northward in segments at a rate overall of approximately 40 mm/a. The rift tip is currently near Mt. Adams (Fig. 1), as inferred from the presence of voluminous Holocene and late Pleistocene low-K tholeiite. Basaltic volcanism has been dominant in southern Washington only for about 1 million years; future structural disruption is therefore expected.

Eruption rates were high during rifting and were highest on the southern, initial end of the rift, but returned to pre-rift levels after the rift passed through. The degree of partial melting was also higher during rifting, as judged from basalt composition (especially Na *versus* Mg; *cf.* Klein & Langmuir 1987). Eruption rates and overall degree of partial melting declined northward along the rift (Conrey *et al.* 1994, Conrey *et al.*, unpubl. data). Post-rift basalt was produced by lower degrees of partial melting and has a distinctly more calc-alkaline or OIB-like character. In this paper, we examine a selection of primitive basalts, both syn- and post-rift, from along the rift (Fig. 1). For comparison, we present data for one primitive basalt from the early Western Cascade arc (Fig. 1). The diversity in K present in our selection of primitive lavas is shown in Figure 2.

ANALYTICAL METHODS

Bulk-rock major-element concentrations were analyzed by X-ray fluorescence (XRF) at either the

TABLE 1. CHEMICAL COMPOSITION OF PRIMITIVE CASCADE ARC BASALTS

Sample	RMC 92-8	RCBD -21	RCBD -41	TED -733	RCGR -236	RCBR -115	RCFB -139	WDS 87-82	CTGH -2576	RCGR -773	RCW -85
Map #	1	2	3	4	5	6	7	8	9	10	11
Lat.	45°36.09'	45°05.70'	45°05.67'	44°33.45'	44°31.01'	44°46.92'	44°50.00'	46°15.94'	44°51.03'	44°31.05'	44°26.29'
Long.	121°59.70'	121°59.87'	122°00.02'	121°17.32'	121°18.60'	121°46.56'	121°40.79'	121°51.28'	121°49.87'	121°37.85'	121°50.29'
Elev.[a]	2400	3040	3040	2300	2600	5460	3770	5000	1264	2780	3700
Type[b]	LKT	LKT	LKT	LKT	LKT	OIB	OIB	OIB	OA	CAB	CAB
Age[c]	3	3	4	6	5	0.3	0.5	<1?	4	0.2	1.2
SiO_2	48.25	47.88	48.49	48.69	50.04	50.75	50.22	48.80	43.71	49.62	52.30
Al_2O_3	16.65	18.25	17.59	17.33	17.84	16.54	16.54	15.89	11.34	15.60	16.48
TiO_2	1.16	0.94	1.05	0.85	0.87	1.57	1.63	1.71	3.59	1.59	1.16
FeO*	11.63	9.12	8.98	9.01	8.67	8.56	8.70	10.05	11.71	10.24	7.63
MnO	0.18	0.16	0.16	0.18	0.17	0.15	0.15	0.16	0.18	0.18	0.14
CaO	9.49	11.43	11.35	12.08	11.15	9.47	9.36	8.90	13.07	9.31	8.80
MgO	9.70	9.63	9.57	9.43	8.53	8.56	8.82	9.94	11.44	9.64	8.84
K_2O	0.09	0.09	0.14	0.11	0.24	0.71	0.77	0.82	0.69	0.47	0.86
Na_2O	2.75	2.39	2.57	2.24	2.39	3.39	3.48	3.35	3.04	2.95	3.52
P_2O_5	0.10	0.09	0.10	0.08	0.09	0.31	0.35	0.38	1.24	0.40	0.26
Mg#	64	69	70	70	68	69	69	68	70	67	72
Ni	208	150	147	152	140	159	165	165	123	223	180
Cr	260	276	272	322	279	304	311	354	410	334	373
Co	57.9			45.0	43.0				55.8		41.3
Sc	30.5	41	39	49.7	40.7	30	31	26	23.3	33	26.0
V	178	210	217	238	232	213	208	200	237	187	196
Ba	71	70	66	89	125	228	245	282	650	220	256
Rb	<1	2	2	3	5	7.8	9	8	45	6	10
Th	0.55	2	1	0.29	0.59	1.63	1		7.20		1.35
U				0.10	0.21	0.52					
Pb	<1	1	<1	0.9	4.4	5.4	<1	2			3
Cs						0.05					
Sr	238	252	263	205	270	578	615	619	1038	701	627
Zr	73	74	82	57	73	143	153	152	401	174	129
Hf	1.85			1.33	1.74	3.27			8.73		2.78
Nb	3.9	2.6	2.7	3.1	2	16.4	18.2	24.2	65	10	10.6
Ta	0.29			0.18	0.17	1.11			3.64		0.56
La	4.7			3.2	5.8	16.2			77		13.4
Ce	12.2			7.7	11.9	35.6	37		154		32.7
Pr				1.3	2.0	4.9					
Nd	20.1			6.5	9.4	21.3			81		15.8
Sm	2.72			1.97	2.58	4.73			16.9		4.16
Eu	0.94			0.81	0.94	1.65			5.15		1.28
Gd				2.77	3.29	4.55					
Tb	0.6			0.48	0.55	0.65			1.4		0.6
Dy				3.48	3.88	4.14					
Ho				0.77	0.87	0.83					
Er				2.48	2.75	2.30					
Tm				0.40	0.45	0.35					
Yb	2.24			2.65	2.95	2.18			2.01		1.87
Lu	0.33			0.43	0.47	0.34					0.25
Y	23	23	24	25.2	25.8	25.7	23	22	36	27	19
Ga	18	17	14	14	13	18	18		19	20	17
Cu	58	49	62	84	109	127	67	53	62	96	56
Zn	85	61	63	56	70	72	70	93	122	102	73

Major-element data are normalized 100%, anhydrous, and expressed in wt %. Samples with full REE data were analyzed for Ba, Th, U, Rb, Cs, Nb, Ta, Hf, Pb, Y, and REE by ICP/MS. Samples with partial REE data were analyzed for Co, Sc, Th, U, Hf, Ta, and several REE by INA. All other data by XRF. Concentrations of trace elements expressed in ppm.
Map # is numbered location in Figure 1.
[a] Elevation in feet; collar elevations for drill core samples CTGH-2576 and 92TB16 are 3840 and 763 feet, respectively.

TABLE 1, CONTINUED

Sample	RCDS -197	92TB 16	DS91 -65	RC-M TBRP	RC-TFJ1	RC-A LDCK	RC93 -50	RMC 92-1	DS90 -47	RC94 -78	RMC NSR-1
Map #	12	13	14	15	16	17	18	19	20	21	22
Lat.	44°23.45'	45°30.57'	46°23.78'	45°30.95'	44°21.70'	45°19.07'	44°35.30'	45°31.39'	46°13.68'	43°20.19'	44°30.72'
Long.	121°32.38'	122°44.20'	121°42.87'	122°35.74'	121°45.64'	122°03.46'	121°20.76'	122°10.92'	121°49.51'	122°13.95'	121°48.87'
Elev.[a]	4920	669	3780	550	4160	3480	1560	1480	3800	4800	420
Type[b]	CAB	CAB	HKCA	HKCA	HKCA	HKCA	AB	AB	AB	DBA	EWCB
Age[c]	2.5	0.9	<0.2	0.5	0.2	2	0.2	1.4	<1	6	33.9
SiO_2	51.38	52.07	50.40	53.44	50.25	50.49	50.18	49.79	50.28	53.50	51.51
Al_2O_3	16.79	16.49	16.49	16.59	16.28	15.21	14.17	15.32	15.27	13.10	15.26
TiO_2	1.42	1.32	1.30	1.20	1.15	1.46	1.55	1.37	1.29	0.59	0.81
FeO*	7.45	8.15	8.40	7.32	8.11	9.13	6.79	8.33	7.22	7.40	8.28
MnO	0.13	0.13	0.14	0.12	0.14	0.15	0.11	0.13	0.11	0.14	0.15
CaO	9.51	8.76	9.74	8.34	9.72	9.63	10.32	10.21	10.44	7.95	10.87
MgO	8.19	7.89	8.52	7.25	9.41	8.68	9.77	8.47	7.84	14.52	10.42
K_2O	1.13	1.20	1.26	1.44	1.43	1.60	3.10	1.76	2.28	0.42	0.39
Na_2O	3.57	3.63	3.31	3.86	3.13	3.21	2.83	3.90	4.36	2.27	2.20
P_2O_5	0.44	0.36	0.42	0.44	0.37	0.44	1.18	0.73	0.89	0.10	0.13
Mg#	71	68	69	69	72	68	77	70	72	81	73
Ni	156	200	156	158	190	164	222	159	194	317	99
Cr	256	327	355	224	341	268	409	251	222	1288	405
Co	39.9	46.8	42.7		43.0	42.6		39.6	39.6		
Sc	23.4	23.5		20	27.1	24.6	20	21.0	19.1	29	39
V	204	196	205	161	177	204	118	205	203	161	225
Ba	552	349	384	671	739	594	2322	1343	1873	89	166
Rb	21	12.6	22	11	6.4	20	30.6	9	11.5	5.6	6
Th	6.06	3.60	4.16	3	0.74	4.17	7.81	3.37	3.76	0.58	2
U	1.65		1.38		0.32	1.70	2.37	0.80		0.21	
Pb	<1			6	5.0	3	14.0	10		1.8	2
Cs					0.12		0.17			0.05	
Sr	924	996	723	1253	1575	1232	3329	3096	3655	641	398
Zr	209	150	190	198	143	189	303	179	194	71	82
Hf	4.76	4.04	4.38		3.68	4.32	7.81	3.90	5.34	1.45	
Nb	10.3	13	14	11.4	4.4	7.7	7.6	9.5	10	2.2	5.6
Ta	0.55	0.88	0.77		0.45	0.63	0.41	0.65	0.55	0.31	
La	37.0	26.5	27.9		21.6	36.4	86.1	56.9	86.4	6.0	
Ce	85.5	63.2	64.6	73	50.8	82.2	191	132	205	12.9	
Pr					7.1		26.8			1.8	
Nd	45.0	25.7	34.1		31.9	51.6	110	57.5	101	7.7	
Sm	8.20	6.20	6.72		6.28	9.05	17.1	11.4	17.3	1.87	
Eu	2.12	1.82	1.89		2.02	2.28	4.43	3.24	4.67	0.7	
Gd					4.41		10.0			1.76	
Tb	0.8	0.4	0.7		0.68	0.8	1.02	0.9	0.9	0.31	
Dy					4.02		4.33			1.83	
Ho					0.77		0.65			0.38	
Er					2.11		1.50			1.08	
Tm					0.28		0.19			0.15	
Yb	1.51	1.46	2.32		1.76	2.03	1.10	1.45	1.44	0.93	
Lu	0.22	0.22	0.31		0.28	0.31	0.16	0.21	0.23	0.14	
Y	21	17	23	20	20.3	22	17	18	19	9.9	14
Ga	17			18	10	16	15	21		13	17
Cu	47	67	62	50	98	45	83	78	91	49	84
Zn	80	81	79	111	74	92	103	108	108	58	72

[b] LKT = low K tholeiite (TED-733 analysis is repeated from Bailey & Conrey [1992]); OIB = OIB-like basalt; OA = olivine analcimite (analysis repeated with updated Nb from Conrey [1990]); CAB = calc-alkaline basalt; HKCA = high-K calc-alkaline basalt; AB = absarokite; DBA = depleted basaltic andesite; EWCB = early Western Cascade basalt.

[c] approximate age in Ma. K-Ar ages are available for samples 11, 12, and 13 (Conrey *et al.* 1996a, 1996b).

Mg# calculated assuming Fe_2O_3/FeO ratio consistent with FMQ buffer (Kress & Carmichael 1991).

Geoanalytical Laboratory of Washington State University (WSU) or at the Geological Survey of Japan (GSJ). At WSU, the analyses were run with 2:1 (flux:rock) lithium tetraborate fused beads and a Rigaku 3370 spectrometer with a Rh target. Operating conditions and standard curves are explained in an internal report from the Geoanalytical Laboratory, available on request. Analyses carried out at the GSJ used 10:1 (flux:rock) lithium tetraborate fused beads and a Philips PW1404 spectrometer with a Sc/Mo dual anode tube. Operating conditions and standards used are contained in several internal reports of the GSJ (in English); copies will be provided on request.

Bulk-rock trace-element concentrations were measured by XRF at both WSU and GSJ, by instrumental neutron activation (INA) at GSJ, and by inductively coupled plasma – mass spectroscopy (ICP–MS) at WSU. In the case of multiple determinations for some elements, only the most reliable data are shown in Table 1. At WSU, concentrations of Cr, Ni, Sc, V, Ba, Rb, Sr, Zr, Nb, Ga, Cu, Zn, Ce, Pb, and Th were determined by XRF on the same fused beads as used for the major elements, whereas the same elements except for Th, Ce, and Ga were determined at GSJ with pressed powder pellets. Minor systematic interlaboratory biases were noted for Ba and Y; some data shown in Table 1 have been adjusted to account for these. Concentrations of rare-earth elements (*REE*), Th, Hf, Ta, Sc, and Co were determined by INA at GSJ. Concentrations of the *REE*, Ba, Nb, Ta, Y, Hf, Th, U, Pb, Rb, and Cs were established by ICP–MS at WSU (methods available on request).

Mineral compositions were measured on a wavelength-dispersion Cameca Camebax electron microprobe at WSU. Both mineral and synthetic standards were used, and all data are ZAF-corrected. Instrument conditions were: an accelerating voltage of 20 kV, beam current of 11.5–13.0 nA, and beam diameter of 2–8 μm (wider for plagioclase). Between four and sixteen cores of olivine phenocrysts were analyzed per sample, with emphasis on the largest phenocrysts, which invariably are the most magnesian. Four to ten augite or plagioclase cores were analyzed in most samples. From two to six spinel inclusions in olivine were analyzed per thin section, depending on abundance. Phlogopite and amphibole were analyzed where present.

PRIMITIVE CASCADE LAVAS

Evaluation of primitive character

Several criteria were used to categorize rocks as primitive. Sparsely porphyritic rocks with Mg# [100 * Mg/(Mg + Fe^{2+}); molar] ≥ 67, calculated with a Fe^{3+}/Fe^{2+} value consistent with $f(O_2)$ at FMQ

TABLE 2. PHENOCRYST ASSEMBLAGES IN PRIMITIVE CASCADE MAGMAS

Sample	Type	Ol	Pl	Cpx	Opx	Hbl*	XCpx#	Phl^	Fo**	An+	AnX++
RMC92-8	LKT	x	tr	–	–	–	–	–	83-84	na	–
RCBD-21	LKT	x	tr	–	–	–	–	–	82-88	81-84	55
RCBD-41	LKT	x	tr	–	–	–	–	–	86-88	na	–
TED-733	LKT	x	–	–	–	–	–	–	85-88	–	58,88
RCGR-236	LKT	x	tr	–	–	–	–	–	81-87	73-77	–
RCBR-115	OIB	X	x	–	–	–	–	tr	81-87	70-77	–
RCFB-139	OIB	x	–	tr	–	–	–	tr	75-84	–	–
WDS87-82	OIB	x	–	–	–	–	–	–	83-86	–	–
CTGH-2576	OA	x	–	X	–	–	–	x	85-88	–	–
RCGR-773	CAB	X	–	–	–	–	–	–	78-88	–	59
RCW-85	CAB	x	tr	–	–	–	–	–	82-86	na	–
RCDS-197	CAB	x	x-mp	x	tr	tr	–	tr	79-86	76	–
92TB16	CAB	x	tr	tr	–	–	–	tr	86-88	na	–
DS91-65	HKCA	x	–	–	–	–	–	–	86-88	–	–
RC-MTBRP	HKCA	x	–	–	–	–	–	–	85-87	–	–
RC-TFJ1	HKCA	X	x	x	–	–	–	tr	76-88	70-83	–
RC-ALDCK	HKCA	x	X-mp	x	–	–	–	tr	83-86	na	–
RC93-50	AB	x	–	x	–	–	–	tr	90-94	–	na
RMC92-1	AB	x	–	x	–	X	tr	tr	87-89	–	–
DS90-47	AB	x	–	x	–	X	tr	x	92-92	–	89
RC94-78	DBA	X	–	x	–	–	–	–	81-90	–	–
RMCNSR-1	EWCB	X	X	X	–	–	–	–	75-88	77-91	–

x - 1-5 %; X - 5-10 %; X - 10-20 %; tr - <1 %; mp - microphenocryst; – not detected; na - detected but not analyzed. *Amphibole is usually relict, converted to opacite. #Brown, turbid, resorbed cores of cpx overgrown by clear, euhedral cpx. ^Groundmass phlogopite (biotite in OA). **Range of Fo content of olivine phenocrysts. +Range of An content of plagioclase phenocrysts (optical determinations for EWCB; all others by microprobe). ++An content of plagioclase xenocrysts.

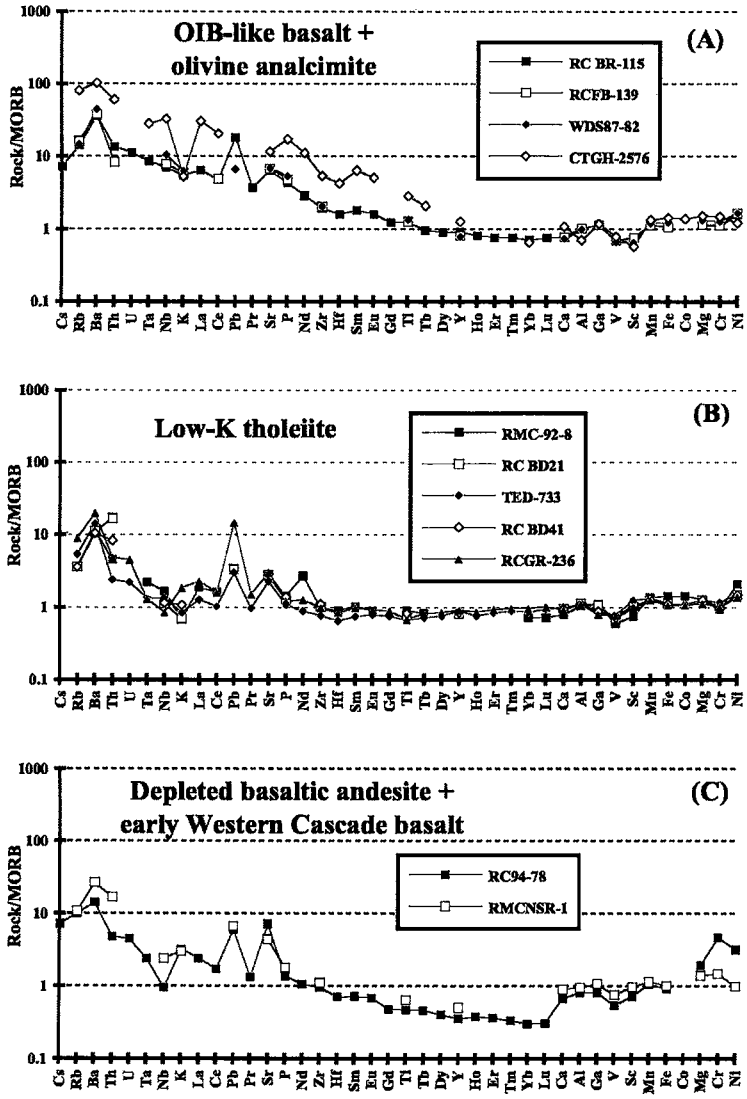

FIG. 3. MORB-normalized spidergrams for Cascade primitive mafic lavas [values for normalization and element ordering from Pearce & Parkinson (1993)]. In D), one sample of shoshonite from Crater Lake (Bacon 1990) and one of "high-Ba – low-HFSE" basalt from Indian Heaven in southwest Washington (Leeman *et al.* 1990) are shown for comparison.

[fayalite – magnetite – quartz oxygen buffer: Kress & Carmichael (1991), that contain olivine phenocrysts having Fo ≥ 86 in equilibrium with the bulk-rock composition are regarded as primitive. These criteria apply to most of the rocks listed in Table 1, including samples of low-K tholeiite from north-central Oregon. However, no samples of low-K tholeiite from northernmost Oregon and southern Washington have a Mg# higher than 64 (Table 1, sample RMC92–8), and we have not found olivine phenocrysts more Mg-rich than Fo_{84} in these rocks (Table 2). However, the most primitive of these northerly low-K tholeiites are nearly aphyric, with ≥9 wt% MgO and ≥200 ppm Ni. The high Fe content of the northernmost low-K tholeiite is consistent with an origin involving melting of deeper mantle than the low-K tholeiite found farther south in north-central Oregon

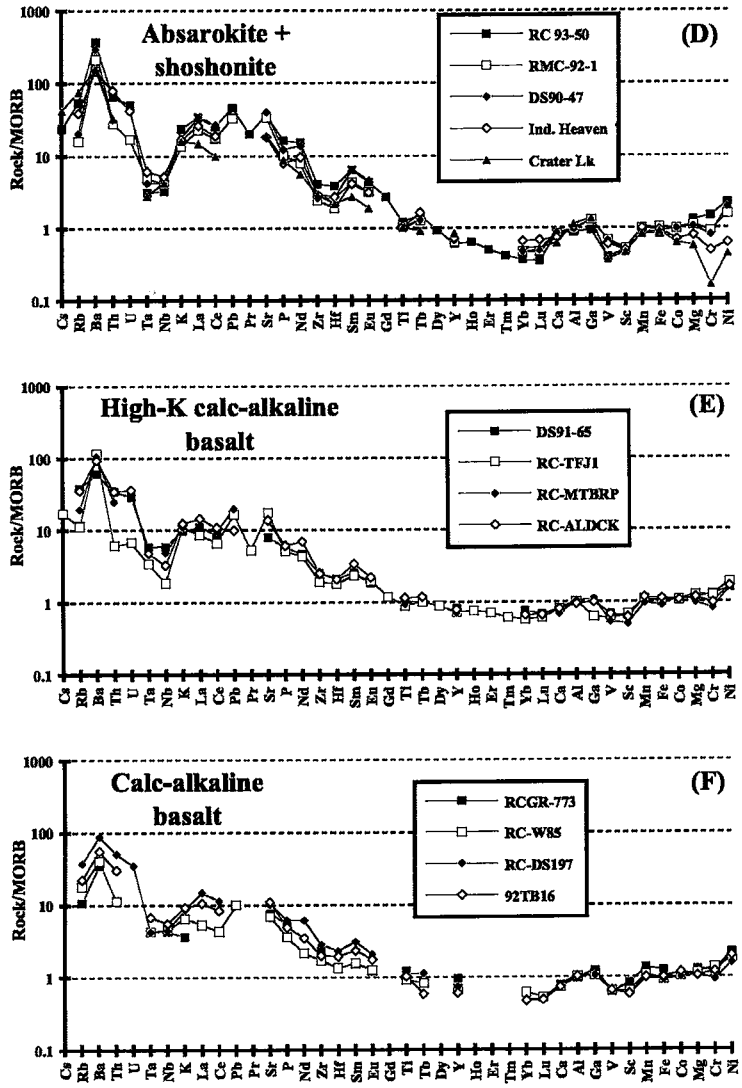

FIG. 3. Cont.

(see *Relation to partial melting*, below). Because the composition of these magmas is consistent with experimental evidence for direct derivation by partial melting of dry peridotite, we regard these northernmost low-K tholeiites as primitive, a conclusion supported by their high Ni concentrations (Sato 1977). More porphyritic samples (*e.g.*, RMCNSR–1) were judged as being primitive if it could be demonstrated that their most Mg-rich phenocrysts were in equilibrium with their Mg-rich bulk-rock composition.

Low-K tholeiite (LKT)

Low-K tholeiite (also called high-alumina olivine tholeiite for their generally high Al content: *e.g.*, Hart *et al.* 1984, Bacon *et al.* 1996), associated with rifting and extension, is common in the Cascades from northern California to southern Washington (Guffanti *et al.* 1990, Bacon 1990, Hughes 1990, Leeman *et al.* 1990). Individual flows of primitive low-K tholeiite lava are the most extensive in the Cascades, commonly covering

100–200 km^2 (Smith 1986, Donnelly-Nolan *et al.* 1991). The samples listed in Table 1 include two from the Deschutes Formation in central Oregon (Smith 1986, Smith *et al.* 1987), two from north of Mt. Jefferson (Fig. 1), and one from the Columbia River Gorge. The two samples near latitude 45°N were collected from the same lava flow at different places; both are presented here to illustrate the precision of our analytical results. There is a change in low-K tholeiite composition near latitude 45°N; to the north, all low-K tholeiite has significantly higher Fe and lower Al than that erupted farther south (Bacon 1990, Leeman *et al.* 1990, Bacon *et al.* 1996, Conrey *et al.*, unpubl. data).

Primitive low-K tholeiite has major-, and trace-element concentrations similar to mid-ocean-ridge basalt (Table 1, Fig. 3). The enrichment in Ba, Th, Pb, and Sr in the Cascade low-K tholeiites (Fig. 3), relative to MORB, has two possible causes: crustal contamination (Bailey & Conrey 1992) or source contamination by subduction. Low-K tholeiite from northernmost Oregon and southern Washington has higher Na and usually lower Sc and heavy *REE* abundances than low-K tholeiite farther south (Table 1; Conrey *et al.*, unpubl. data, Bacon *et al.* 1996).

Primitive low-K tholeiite lavas contain sparse phenocrysts of olivine and traces of plagioclase phenocrysts (Table 2), typically in a medium-grained, subophitic, diktytaxitic groundmass. The olivine crystals are normally zoned; phenocryst cores range from Fo_{81} to Fo_{88} (Tables 2, 3). The most Fo-rich cores are usually the largest (2–3 mm). Olivine in low-K tholeiite has between 0.20 and 0.33 wt% CaO and ≤ 0.23 wt% NiO, although Ni data are limited. Spinel is common as an inclusion in olivine phenocryst, and is locally preserved outside the olivine crystals. Spinel in primitive low-K tholeiite has a Cr# [Cr/(Cr + Al); molar] in the range from 0.13 to 0.29 (Table 4, Fig. 4), the lowest in the Cascade arc, similar to Cr-poor spinel in MORB (Dick & Bullen 1984, Roeder 1994).

Traces of plagioclase phenocrysts are usually present in primitive low-K tholeiite (Tables 2, 5); analyzed crystals are An_{73}–An_{84}. These crystals commonly are skeletal and contain inclusions of trapped minerals and melt. Megacrysts of more calcic plagioclase ($An_{84–88}$) are found in some samples; these seem to correspond to megacrysts of highly calcic plagioclase found in MORB (Donaldson & Brown 1977). Rare reversely zoned xenocrysts (with cores of An_{55} to An_{60}) are present in some samples. These probably represent contaminants, as they are too sodic to be relics of high-pressure crystallization (Panjasawatwong *et al.* 1995).

OIB-like basalt (OIB)

Two small flows of primitive basalt with OIB-like chemical character (Table 1, Fig. 3) are known north of Mt. Jefferson (Fig. 1) in a post-rift setting. The other sample of primitive OIB-like basalt is from a dike (Swanson 1991) near the present tip of the rift in southern Washington. These rocks have a composition like that of OIB, with higher overall concentrations of incompatible elements than low-K tholeiite (Fig. 3). Nb anomalies are absent in these rocks (Fig. 3). Lower levels of Sc, Y and heavy *REE* than in low-K tholeiite are notable, as are lower Ca and higher Si (Table 1). Near-primitive basalt with a composition intermediate between low-K tholeiite and OIB-like basalt also is known from northernmost Oregon.

OIB-like basalts contain sparse to modest (~2 to 8%) amounts of olivine phenocrysts, in some cases accompanied by plagioclase and rarely by clinopyroxene, in a fine-grained intergranular groundmass that commonly contains traces of phlogopite (Tables 2, 6). The cores of olivine phenocrysts range from Fo_{75} to Fo_{87} and are normally zoned. Olivine in OIB-like basalt contains 0.15–0.27 wt% CaO (lower than in olivine from low-K tholeiite); no data on Ni concentration are available. Spinel inclusions in olivine in OIB-like basalt have Cr# between 0.30 and 0.62, distinctly higher than in spinel from low-K tholeiite, but similar to that in spinel in calc-alkaline basalt and high-K calc-alkaline basalt (see below; Table 4, Fig. 4). Spinel in Cascade OIB-like basalt also is similar to spinel in oceanic OIB (Roeder 1994). Plagioclase phenocrysts in sample RCBR–115 range from An_{70} to An_{77} (Tables 2, 5).

Olivine analcimite (OA)

One sample of olivine analcimite (equivalent to olivine nephelinite but with analcime, not nepheline, present in the groundmass) lava with extreme OIB-like character is known from drill core north of Mt. Jefferson (Table 1, Fig. 3; Conrey 1990). The petrology of this sample has already been reported, but is included here for comparison. The analcimite contains phenocrysts of olivine and clinopyroxene in a very fine-grained groundmass [Table 2; see Conrey (1990) for compositions]. The olivine has the highest Ca content (≤0.40 wt% CaO) of any olivine in the Cascades. Clinopyroxene compositions define a trend toward increasing Wo content (Fig. 5), typical of pyroxene in such silica-undersaturated rocks. Compositions of clinopyroxene phenocrysts have increasing Ti with decreasing En content (mol%; not shown). They also have low Na and ^{VI}Al. Spinel inclusions in olivine have a Cr# similar to those in OIB-like basalt, calc-alkaline basalt, and high-K calc-alkaline basalt spinel (see below; Fig. 4).

Calc-alkaline basalt (CAB)

Primitive basalts with trace-element patterns typical of calc-alkaline lavas (Fig. 3) are found in several places in northern Oregon (Fig. 1). Most of these rocks were erupted post-rift, but some were erupted syn-rift in northernmost Oregon and southern Washington. The major-element concentrations are broadly similar to

TABLE 3. REPRESENTATIVE COMPOSITIONS OF OLIVINE, NORTHERN CASCADE ARC

SAMPLE	Point	SiO_2	TiO_2	Al_2O_3	Cr_2O_3	MgO	FeO	CaO	NiO	MnO	Na_2O	K_2O	Total	Fo
TED-733	16	40.17	0.00	0.09	0.06	47.30	11.42	0.27	0.23	0.22	--	--	99.77	88.1
RCBD-21	49	40.10	0.02	0.05	--	47.66	11.38	0.24	--	0.14	0.04	0.00	99.63	88.2
RCBD-41	58	40.63	0.00	0.07	--	47.53	11.67	0.25	--	0.16	0.03	0.00	100.36	87.9
RCGR-236	100	40.27	0.00	0.09	0.00	46.64	12.42	0.22	0.16	0.17	--	--	99.96	87.0
RCBR-115	110	40.66	0.02	0.04	--	47.05	12.06	0.17	--	0.11	0.03	0.01	100.15	87.4
WDS87-82	179	39.55	0.01	0.00	--	45.87	13.64	0.17	--	0.14	0.00	0.01	99.40	85.7
92TB16	15	40.59	0.00	0.00	--	46.52	11.89	0.12	--	0.19	0.01	0.01	99.34	87.5
RCW-85	92	39.42	0.03	0.05	0.05	45.19	13.64	0.14	0.23	0.23	--	--	98.99	85.5
RCGR-773	39	39.83	0.00	0.03	0.04	47.04	11.80	0.15	0.33	0.17	--	--	99.39	87.7
RC-MTBRP	52	39.93	0.01	0.03	--	46.69	12.18	0.11	--	0.23	0.00	0.00	99.18	87.2
DS91-65	187	39.80	0.02	0.02	--	47.22	11.40	0.15	--	0.14	0.02	0.00	98.78	88.1
RC-TFJ1	42	40.26	0.04	0.04	0.04	47.25	11.81	0.20	0.23	0.19	--	--	100.06	87.7
DS90-47	59	41.06	0.01	0.01	--	50.72	7.42	0.20	0.15	0.47	0.05	0.00	99.95	92.4
RMC92-1	77	40.41	0.01	0.00	--	48.12	10.95	0.20	--	0.30	0.03	0.00	100.03	88.7
RC93-50	19	40.58	0.01	0.03	--	51.10	6.80	0.15	--	0.13	0.04	0.01	98.84	93.1
RC93-50	20	41.22	0.01	0.04	--	51.82	5.73	0.18	--	0.27	0.01	0.00	99.28	94.2
RC94-78	28	39.77	0.03	0.03	0.03	49.14	9.82	0.08	0.25	0.17	--	--	99.30	89.9
RC94-78	30	40.31	0.00	0.05	0.04	48.68	10.42	0.10	0.31	0.10	--	--	100.01	89.3
RMCNSR-1	76	39.96	0.01	0.02	0.00	48.03	11.81	0.15	0.13	0.15	--	--	100.25	87.9

All data from cores except point #20 is rim of core #19. -- not analyzed. Major element proportions expressed as oxides in wt. %.

TABLE 4. REPRESENTATIVE COMPOSITIONS OF SPINEL, NORTHERN CASCADE ARC

Sample	Point	SiO_2	TiO_2	Al_2O_3	Cr_2O_3	V_2O_3	MgO	FeO	NiO	MnO	ZnO	CaO	Total	Mg#	Cr#	Fe3#
TED-733	99	0.06	0.19	48.68	16.47	0.19	18.98	14.83	0.18	0.25	--	--	99.84	0.76	0.18	0.05
RCGR-236	10	0.23	0.27	41.39	18.61	0.18	14.04	25.41	0.17	0.32	--	--	100.63	0.59	0.23	0.10
RCBD-41	10	0.17	0.16	51.17	14.33	0.08	20.01	14.47	0.20	0.21	--	--	100.78	0.79	0.16	0.05
RCBD-21	6	0.18	0.19	52.91	12.80	0.11	20.00	13.23	0.28	0.14	--	--	99.83	0.79	0.14	0.04
RCFB-139	86	0.15	0.77	25.37	24.69	0.16	9.21	35.92	0.18	0.44	--	--	96.91	0.43	0.39	0.20
RCBR-115	23	0.21	0.81	31.75	28.12	0.17	13.94	23.98	0.22	0.34	--	--	99.54	0.61	0.37	0.10
WDS87-82	44	0.18	1.04	33.96	23.73	0.20	14.65	25.44	0.18	0.34	--	--	99.72	0.63	0.32	0.12
92TB16	55	0.29	1.25	22.28	31.20	0.17	11.77	29.64	0.24	0.41	--	--	97.23	0.55	0.48	0.17
RCDS-197	62	0.18	0.81	11.38	23.59	0.11	8.53	50.06	0.33	0.39	--	--	95.38	0.43	0.58	0.44
RCW-85	27	0.17	0.59	16.61	32.08	0.31	8.97	34.31	0.27	0.42	0.21	0.04	93.99	0.46	0.56	0.22
RCGR-773	30	0.20	1.02	28.39	31.18	0.14	14.62	24.17	0.23	0.40	--	--	100.36	0.64	0.42	0.12
RC-MTBRP	7	0.22	1.07	21.49	33.30	0.13	13.17	28.30	0.31	0.36	--	--	98.36	0.60	0.51	0.17
DS91-65	51	0.17	0.84	29.66	29.96	0.13	14.52	23.18	0.27	0.36	--	--	99.10	0.64	0.40	0.11
RC-ALDCK	73	0.14	1.75	18.44	28.77	0.16	8.73	38.89	0.19	0.49	--	--	97.58	0.41	0.51	0.24
RC-TFJ1	44	0.22	0.64	31.76	29.26	--	14.39	23.21	0.18	0.30	--	0.01	99.97	0.63	0.38	0.10
RMC92-1	68	0.25	1.11	11.20	29.60	0.16	9.12	43.35	0.38	0.43	--	--	95.60	0.46	0.64	0.36
RC93-50	22	0.22	0.74	6.49	22.26	0.03	11.19	52.28	0.54	0.36	--	--	94.11	0.57	0.70	0.55
RC94-78	15	0.23	0.12	6.86	50.99	0.06	7.87	29.85	0.14	0.55	0.21	0.02	96.91	0.42	0.83	0.15
RMCNSR-1	19	0.18	0.35	18.61	38.06	0.19	10.35	28.40	0.09	0.49	0.14	0.02	96.88	0.51	0.58	0.14

All compositions pertain to cores of inclusions in olivine. -- not analyzed. Mg#, etc. calculated using Cameca Strucgeo stoichiometry.

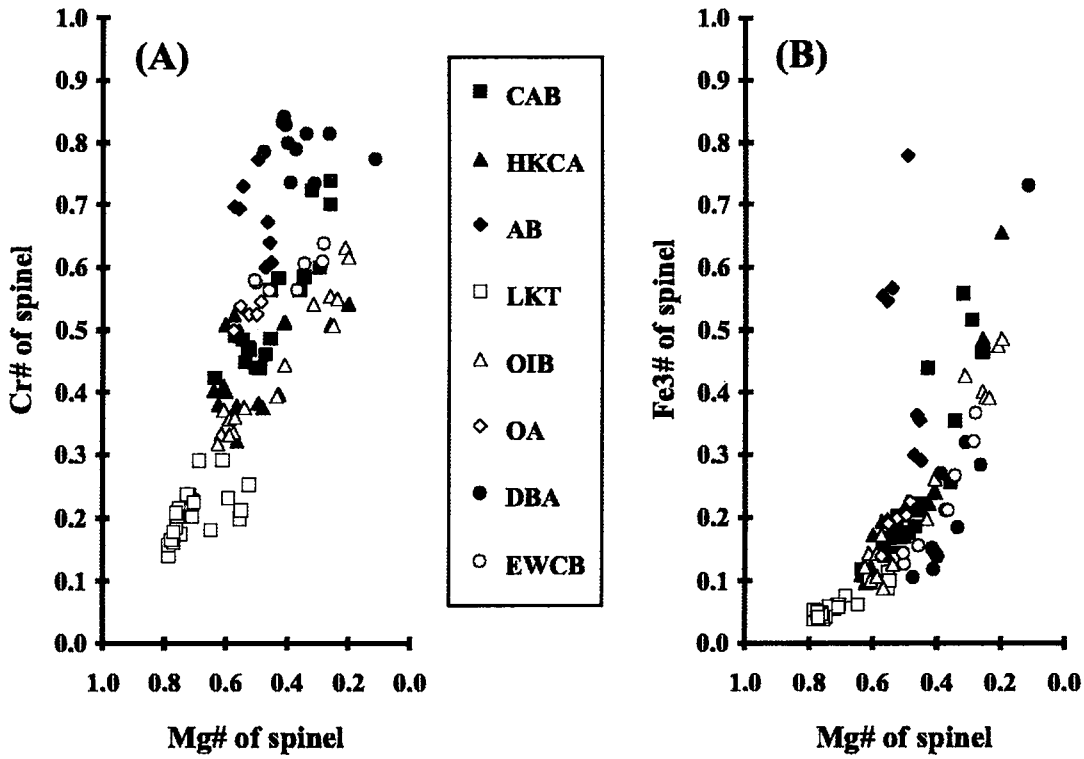

FIG. 4. Chemistry of spinel in primitive Cascade lavas. A) Cr# [Cr/(Cr + Al)] *versus* Mg# [Mg/(Mg + Fe^{2+})] of spinel. B) Fe3# [Fe^{3+}/(Fe^{3+} + Al + Cr)] *versus* Mg# [Mg/(Mg + Fe^{2+})] of spinel. Note that Mg# of spinel and Mg# of bulk-rock compositions are not identical.

TABLE 5. REPRESENTATIVE COMPOSITIONS OF PLAGIOCLASE, NORTHERN CASCADE ARC

Sample	Point	SiO_2	TiO_2	Al_2O_3	FeO	CaO	MgO	MnO	BaO	Na_2O	K_2O	Total	An	Ab	Or
TED-733	95	46.42	--	34.04	0.39	18.01	--	--	0.01	1.35	0.01	100.23	88.0	11.9	0.1
TED-733	97	54.12	--	28.33	0.93	11.92	--	--	0.02	4.60	0.19	100.11	58.2	40.7	1.1
RCGR-236	41	49.07	--	31.61	0.98	15.24	--	--	0.00	2.47	0.06	99.44	77.0	22.6	0.4
RCBD-21	47	54.45	0.03	28.05	0.57	11.35	0.17	0.03	--	5.03	0.13	99.82	55.1	44.2	0.8
RCBD-21	56	47.04	0.00	33.01	0.49	17.19	0.12	0.00	--	1.80	0.02	99.66	84.0	15.9	0.1
RCBD-21	57	48.02	0.05	32.65	0.50	16.15	0.15	0.01	--	2.12	0.04	99.70	80.6	19.1	0.2
RCBR-115	120	48.11	0.05	31.98	0.46	16.15	0.15	0.00	--	2.57	0.05	99.53	77.4	22.3	0.3
RCBR-115	123	50.06	0.07	31.14	0.52	14.63	0.12	0.00	--	3.40	0.11	100.05	70.0	29.4	0.6
RCGR-773	162	54.49	--	28.56	0.69	11.81	--	--	0.00	4.47	0.17	100.19	58.8	40.2	1.0
RCDS-197	25	48.03	0.06	31.94	0.51	15.44	0.07	0.00	--	2.62	0.10	98.76	76.1	23.4	0.6
RC-TFJ1	106	47.56	--	33.02	0.69	16.58	--	--	0.04	1.82	0.08	99.79	83.0	16.5	0.5
RC-TFJ1	107	48.53	--	32.44	0.68	15.51	--	--	0.03	2.37	0.10	99.66	77.9	21.5	0.6
RC-TFJ1	108	50.00	--	31.31	0.63	14.69	--	--	0.01	2.89	0.18	99.69	73.0	26.0	1.1
DS90-47	54	45.40	0.01	34.43	0.26	17.94	0.03	0.03	--	1.21	0.04	99.35	88.9	10.9	0.2
DS90-47	55	56.80	0.13	25.78	0.87	7.61	0.02	0.03	--	6.16	1.05	98.44	38.0	55.7	6.2

All data are from cores or prominent mantles. -- not analyzed. Points 97, 47, and 162 are from reversely-zoned xenocrysts. Point 95 is from calcic megacryst. Point 54 is from calcic xenocryst (high-pressure phenocryst?), mantled by point 55 andesine. All other data are from phenocrysts.

TABLE 6. REPRESENTATIVE COMPOSITIONS OF PHLOGOPITE AND AMPHIBOLE, NORTHERN CASCADE ARC

Sample	Point	SiO_2	TiO_2	Al_2O_3	MgO	FeO	CaO	MnO	Na_2O	K_2O	Total
RCBR-115	124	40.42	4.49	12.16	21.13	5.65	0.04	0.05	0.91	8.97	93.83
RC-TFJ1	17	40.19	4.58	11.80	19.73	8.14	0.06	0.12	1.00	9.13	94.77
RC-ALDCK	81	39.86	5.60	12.42	20.32	6.17	0.03	0.04	0.87	8.98	94.28
DS90-47	60	37.83	8.60	13.49	19.04	5.57	0.06	0.11	0.92	8.66	94.28
RCDS-197	27	46.87	1.93	7.16	18.42	6.51	11.09	0.17	2.69	1.18	96.02
DS90-47	41	42.23	2.49	12.29	16.44	7.60	11.78	0.08	3.12	1.22	97.25
DS90-47	47	41.43	5.60	11.17	15.75	6.94	11.87	0.12	2.73	1.29	96.90

All data from cores. Points 124, 17, 81, and 60 are from groundmass phlogopite. Point 47 is from groundmass kaersutite. Point 27 is edenite intergrown with point 28 augite (table 7). Point 41 is the best preserved relict pargasite in DS90-47.

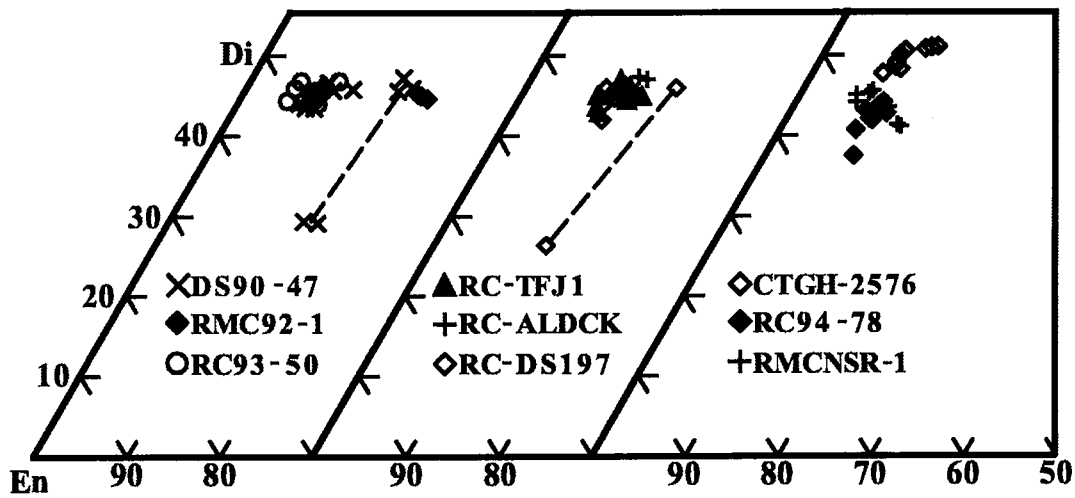

FIG. 5. Pyroxene and amphibole compositions (molar proportions) of primitive Cascade lavas, plotted on magnesian part of pyroxene quadrilateral. Tie-line for DS90–47 indicates possible equilibrium between high-pressure, more Fe-rich augite and resorbed amphibole. Tie-line for RC–DS197 indicates equilibrium between low-pressure, more Fe-rich augite and amphibole in intergrowth. Sample RC–DS197 also contains equilibrium(?) orthopyroxene (En_{78}).

those in OIB-like basalt, with the exception of lower FeO* and TiO_2, and higher SiO_2 and K_2O (Table 1). The trace-element abundances of calc-alkaline basalt and OIB-like basalt are broadly similar as well (Fig. 3). However, trace-element abundance patterns of calc-alkaline basalts have distinct but modest depletions in Ta and Nb compared to the other *LILE* (Fig. 3). Primitive calc-alkaline basalt has relatively constant Nb content, distinctly lower than in OIB-like basalt, but their *LILE* concentrations (*e.g.*, Th, La) are somewhat variable (Fig. 3).

All samples of calc-alkaline basalt contain phenocrysts of olivine, usually sparse plagioclase phenocrysts or microphenocrysts, and, locally, augite (Table 2). The groundmass texture is typically fine-grained intergranular, and traces of phlogopite are commonly present (Table 2). Olivine phenocrysts range in composition from Fo_{78} to Fo_{88} and are normally zoned. Olivine contains low Ca (0.11–0.22 wt% CaO), in agreement with the low Ca content of the bulk rocks. The olivine has rather high Ni concentrations, from 0.15 to 0.33 wt% NiO. Spinel in olivine has a Cr# between 0.42 and 0.74, a range similar to but slightly higher than that in OIB-like basalt (Fig. 4, Table 4). Most augite in calc-alkaline basalt sample RCDS–197 is Mg-rich, but one augite crystal intergrown with amphibole, magnetite, and ilmenite is more Fe-rich (Tables 6, 7, Fig. 5). The amphibole in this intergrowth is too Al-poor to be in equilibrium with the bulk rock (Sisson & Grove 1993a), and the crystal cluster likely is xenocrystic.

TABLE 7. REPRESENTATIVE COMPOSITIONS OF PYROXENES, NORTHERN CASCADE ARC

Sample	Point	SiO_2	TiO_2	Al_2O_3	Cr_2O_3	MgO	FeO	CaO	NiO	MnO	Na_2O	K_2O	Total	Wo	En	Fs
RCDS-197	31	50.27	0.85	4.60	--	15.46	5.24	21.65	--	0.08	0.40	0.01	98.56	45.8	45.5	8.7
RCDS-197	28	52.09	0.28	1.26	--	13.13	9.85	21.90	--	0.34	0.32	0.00	99.15	45.8	38.2	16.1
RCDS-197	199	55.46	0.46	0.85	--	29.22	12.55	1.48	--	0.42	0.03	0.02	100.49	2.9	78.3	18.9
RC-ALDCK	83	48.91	1.40	5.60	--	13.86	6.94	22.25	--	0.09	0.41	0.00	99.45	47.4	41.1	11.5
RC-TFJ1	39	51.76	0.61	2.74	0.42	16.64	5.36	21.20	0.05	0.17	--	--	98.96	43.7	47.7	8.6
RC-TFJ1	26	49.27	1.14	5.61	0.53	14.78	5.94	22.06	0.01	0.09	--	--	99.43	46.7	43.5	9.8
DS90-47	42	50.78	0.34	4.17	--	12.36	9.97	20.72	--	0.26	0.85	0.00	99.44	45.3	37.6	17.0
DS90-47	43	51.23	0.70	3.37	--	15.67	4.62	22.36	--	0.15	0.46	0.00	98.55	46.8	45.6	7.6
RMC92-1	65	50.22	0.40	4.35	--	11.84	11.03	20.61	--	0.28	0.76	0.01	99.50	45.1	36.0	18.8
RMC92-1	66	51.91	0.52	3.37	--	16.35	4.88	21.27	--	0.12	0.51	0.00	98.92	44.5	47.6	8.0
RC93-50	10	52.66	0.60	1.66	--	17.68	3.99	22.17	--	0.12	0.28	0.00	99.16	44.5	49.3	6.2
RC93-50	29	54.27	0.29	2.93	--	32.55	6.79	1.72	--	0.11	0.04	0.01	98.71	3.3	86.6	10.1
RC94-78	11	53.15	0.22	1.62	0.45	18.94	5.99	18.70	0.00	0.19	--	--	99.27	37.6	53.0	9.4
RC94-78	25	52.45	0.34	2.84	0.50	16.88	5.21	21.46	0.01	0.16	--	--	99.86	43.8	47.9	8.3
RMCNSR-1	67	51.35	0.49	2.93	0.21	16.35	7.75	20.00	0.00	0.23	--	--	99.31	41.0	46.6	12.4
RMCNSR-1	75	52.47	0.22	2.67	0.47	17.22	3.99	22.21	0.02	0.07	--	--	99.34	45.1	48.6	6.3

All data from cores. -- not analyzed. Point 28 is from augite intergrown with edenite (see table 6). Points 39 and 26 are from different sectors of sector zoned crystals. Points 42 and 65 are from brown, resorbed cores surrounded by clear, euhedral augite (points 43 and 66). Point 29 is inclusion in Fo92 olivine.

Sample RCDS–197 also contains rare equilibrium(?) orthopyroxene (En_{78}; Table 7), and rare xenocrysts of orthopyroxene ($Wo_{1.8}En_{62}$) mantled by Mg-rich augite. Only sparse data are available on plagioclase in samples of primitive calc-alkaline basalt: sample RCDS–197 has An_{76} microphenocrysts, whereas sample RCGR–773 has partly resorbed An_{59} xenocrysts, similar to those found in low-K tholeiite (Tables 2, 5).

High-K calc-alkaline basalt (HKCA)

Primitive calc-alkaline basalt with more pronounced "calc-alkaline" trace-element signatures and higher levels of K (> 1.25 wt% K_2O) than typical calc-alkaline basalt (Figs. 2, 3) is here termed high-K calc-alkaline basalt (HKCA). These rocks were erupted in similar tectonic conditions to calc-alkaline basalt: usually post-rift, but in some cases syn-rift in northernmost Oregon and southern Washington. The major-element composition of high-K calc-alkaline basalt is similar to that of calc-alkaline basalt, but the subduction-related trace-element signature is intermediate between that of calc-alkaline basalt and absarokite (Fig. 3; see below). As with calc-alkaline basalt, there is variability in the enrichment of some *LILE*, especially Th, U, and Rb (Table 1, Fig. 3), which can fall in the range from 6 to 40 times typical MORB concentrations.

High-K calc-alkaline basalt samples invariably contain olivine phenocrysts, and commonly plagioclase and augite as well, in a fine-grained intergranular groundmass that typically contains minor phlogopite (Tables 2, 6). Olivine phenocrysts are normally zoned and range from Fo_{76} to Fo_{88}; the widest range in composition is found in the most porphyritic samples (Tables 2, 3). The olivine contains from 0.11 to 0.27 wt% CaO, similar to calc-alkaline basalt, whereas the level of Ni is ≤0.23 wt% NiO, distinctly lower than in calc-alkaline basalt, but based on limited data. Spinel inclusions in olivine have a Cr# from 0.32 to 0.54 (Fig. 4, Table 4), which overlaps the range found in spinel in OIB-like basalt. Augite phenocrysts in high-K calc-alkaline basalt are Mg-rich, but slightly more Fe-rich on average than augite in absarokite (Fig. 5, Table 7). All of the augite phenocrysts are sector-zoned: the more Mg-rich and Ca-poor sectors contain considerably less Al, Cr, and Ti than adjacent sectors (Table 7). The ^{VI}Al content (0.01–0.09 atoms per formula unit [*apfu*]) of high-K calc-alkaline basalt augite is strongly affected by sector zoning, and high ^{VI}Al is not accompanied by high Na (≤0.04 *apfu*; most ≤0.03 *apfu*). The range in Cr content in augite in high-K calc-alkaline basalt is similar to that found in augite in depleted basaltic andesite and early Western Cascade basalt (0.009–0.025 *apfu*; see below). Plagioclase phenocrysts in high-K calc-alkaline basalt sample RC–TFJ1 span the range An_{70} to An_{83} (Tables 2, 5). Traces of xenocrystic quartz also are present in samples RC–TFJ1 and DS91–65, and are commonly found in high-K calc-alkaline basalt and absarokite. Quartz xenocrysts are common in calc-alkaline lamprophyres (Rock 1984), the compositional equivalents of shoshonite and absarokite.

Absarokite (AB)

Several small flows of absarokite, with the most characteristic trace-element signatures of subduction-zone magmas in the Cascades (*i.e.*, largest relative depletions in *HFSE* compared to *LILE*; Table 1, Fig. 3), have

been discovered. They are here called absarokite because of their high K contents (> 1.75 wt% K_2O; Fig. 2) and lack of plagioclase phenocrysts (Table 2; Iddings 1895, Gill & Whelan 1989). One flow (with a part of its vent preserved) was erupted in the Western Cascades in Oregon west of the main axis of Quaternary volcanism (Fig. 1). Another is from a small vent near the Columbia River in Oregon, whereas the third is near the tip of the rift in Washington. All these lavas are of Quaternary age (Table 1). Absarokite is similar to, but more primitive than, shoshonite from Crater Lake (Bacon 1990) and "high-Ba, low-*HFSE* basalt" from southern Washington (Leeman *et al.* 1990; Fig. 3). Absarokite may be the parent of shoshonite in the Cascades.

Samples of absarokite contain phenocrysts of olivine and augite, and generally abundant relict amphibole, set in a very fine-grained intergranular groundmass (Tables 2, 3, 6, 7). Sample DS90–47 has sparse olivine. The olivine in these rocks is the most Mg-rich in the Cascades (Fo_{87} to Fo_{94}). The crystals are usually slightly reversely zoned, and have high Mn contents, especially toward the rim (Fig. 6). The concentration of Ca is low in olivine from absarokite (0.10–0.20 wt% CaO). The Ni content in olivine (≤ 0.17 wt% NiO) also is lower than in high-K calc-alkaline basalt, but data are sparse. The spinel included in olivine is Cr-rich, with a Cr# from 0.60 to 0.78 (Table 4, Fig. 4). It is consistently more Fe^{3+}-rich than that in other Cascade rocks (Fig. 4).

Augite phenocrysts are Mg-rich (Table 7, Fig. 5). In the two samples containing relict amphibole, Mg-rich augite commonly contains a rounded, resorbed core of brown, turbid, more Fe-rich augite (Table 7, Fig. 5). Such augite has an appropriate Mg# to be in equilibrium with relict amphibole (Fig. 5). Augite phenocrysts in the two samples with such relict cores have higher ^{VI}Al contents (0.42–0.76 *apfu*) than augite in sample RC93–50 (≤ 0.42 *apfu*).

Relics of amphibole, now mostly "opacite", are abundant in two samples of absarokite (Tables 2, 6). As noted above, these could have crystallized in equilibrium with more Fe-rich augite. Relict amphibole has the correct Al/Si value to be in equilibrium with the host rock (Sisson & Grove 1993a), but the Fe/Mg value is too high. Sample DS90–47 contains rare fragments of hornblende gabbro composed of 45% plagioclase ($\geq An_{80}$ in the core with an abrupt sodic mantle) and 40% amphibole (largely converted to "opacite"). Minor components include augite (2–3%), phlogopite (2–3%), pseudobrookite(?) (1%), and traces of olivine(?) and apatite. All grains are in contact with 10% interstitial brown glass. The composition (similar trace-element pattern to the host, but at about one-third the concentration; not shown) and mineralogy of the gabbro strongly suggest a genetic relationship with the host rock. The resemblance of the relict amphibole phenocrysts to amphibole in the gabbro suggests that the former are derived by disaggregation of the gabbro. Rare xenocrysts of highly calcic plagioclase mantled by andesine in sample DS90–47 (Tables 2, 5) could be derived the same way.

Absarokite sample RC93–50 contains rare xenoliths of medium-grained granitic rocks and partially resorbed xenocrysts of sodic plagioclase (Table 2) derived from disaggregation of the xenoliths. This contamination

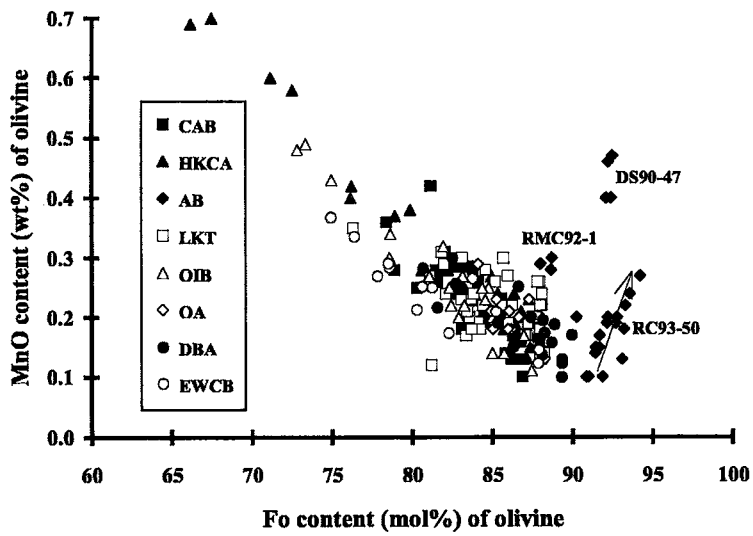

FIG. 6. MnO content (wt%) *versus* Fo (mol.%) of phenocryst and groundmass olivine in primitive lavas. Absarokite sample numbers are given next to data clusters. Arrow shows trend of reverse zoning and increase in MnO in olivine of sample RC93–50.

probably occurred at a relatively shallow depth, as it is not reflected in higher ^{VI}Al and Na contents in the augite phenocrysts (see discussion of intensive parameters below). One grain of olivine in sample RC93–50 contains inclusions of orthopyroxene (En_{87}; Table 7) and sanidine (too small for reliable analysis). These features may result from nucleation of olivine by reaction with low-pressure contaminants, because the enstatite has low Na and ^{VI}Al contents (Table 7; see discussion below).

Early Western Cascade basalt (EWCB)

A lava with primitive characteristics has been found during a reconnaissance study of the older Western Cascades (Fig. 1). A sample from the same outcrop yielded a K–Ar age of 33.9 ± 0.8 Ma (Lux 1982). The flow is compositionally similar to that of more recent calc-alkaline basalt by way of its high SiO_2 and low Al_2O_3, but the low K_2O and trace-element content of the early Western Cascade basalt are more like low-K tholeiite, not calc-alkaline basalt. There is no modern equivalent to this rock in the Cascades. The trace-element pattern is distinctly indicative of a calc-alkaline affinity and similar to that of depleted basaltic andesite (Fig. 3; see below).

The early Western Cascade basalt is abundantly porphyritic and contains phenocrysts of plagioclase, olivine, and augite in a fine-grained groundmass (Table 2). The phenocryst assemblage is similar to those of calc-alkaline and high-K calc-alkaline basalt, but the abundance of phenocrysts in the older rock is notable. Olivine phenocrysts span the range Fo_{75} to Fo_{88}, and the crystals are normally zoned (Tables 2, 3). The Ca content of olivine is low, from 0.10 to 0.16 wt% CaO, and Ni (≤0.15 wt% NiO) is low as well. Spinel inclusions in olivine have a Cr# near 0.60 (Fig. 4, Table 4). The augite is Mg-rich, similar to augite in absarokite (Fig. 5, Table 7). Plagioclase compositions (determined by optical methods with Carlsbad–albite twins) are An_{77} to An_{91}. The presence of anorthite phenocrysts in Western Cascade mafic lavas has been previously established by electron-microprobe analysis (Ritchie 1987).

Depleted basaltic andesite (DBA)

After a diligent search in the Western Cascades, one unusual primitive basaltic andesite lava was found (Fig. 1, Table 1). The search was undertaken because similar lavas are common in the Quaternary Cascades of northern California (M. Clynne, pers. comm., 1993). The depleted basaltic andesite lava found in northern Oregon is in a sequence of mafic lavas that caps ridges in the Western Cascades. These ridge-capping lavas in northern Oregon were erupted concurrently with intra-arc rifting and are late Miocene and Pliocene in age. The late Miocene – Pliocene tectonic setting of northern Oregon was similar to that of the Quaternary Cascades of northern California, where Basin-and-Range extension and voluminous eruption of low-K tholeiite have occurred within the arc (Guffanti *et al.* 1990). Similar high-Mg andesites, commonly coeval with intra-arc or backarc rifting, are erupted in forearcs and near-arc volcanic fronts (Tatsumi & Maruyama 1989).

The composition of depleted basaltic andesite is similar to that of primitive basaltic andesite in northern California (Baker *et al.* 1994). Depleted basaltic andesite there commonly was emplaced near the volcanic front. These basaltic andesites have low Al_2O_3 and incompatible trace-element contents (Table 1, Fig. 3), especially of the heavy *REE*. The trace-element character is distinctly calc-alkaline, similar to early Western Cascade basalt (Fig. 3).

Depleted basaltic andesite contains abundant olivine and sparse augite phenocrysts in a very fine-grained groundmass (Table 2). Olivine phenocrysts range in composition from Fo_{90} to Fo_{81} (Tables 2, 3) and are normally zoned. The Ca content in olivine is decidedly low, from 0.08 to 0.15 wt% CaO, whereas Ni is high (≤0.34 wt% NiO). The spinel is the most Cr-rich known in the northern Cascades, with a Cr# of approximately 0.80 (Fig. 4, Table 4). The Fe3# [$Fe^{3+}/(Fe^{3+} + Al + Cr)$; molar] of spinel in depleted basaltic andesite is slightly lower than is typical of the other primitive basalts (Fig. 4). Such Cr-rich and Fe^{3+}-poor spinel is similar to spinel in boninite (Roeder 1994). Augite is Mg-rich, but slightly less Ca-rich than augite in absarokite, high-K calc-alkaline basalt, or early Western Cascade basalt (Fig. 5, Table 7).

Discussion

Assessment of equilibrium

One goal of igneous petrology is to use observational and experimental data to make inferences about the intensive parameters of magmas. Such inferences are possible only if it can be shown that the rocks and minerals in question approximate experimentally determined equilibrium relationships between liquid and crystals. In this case, we propose using the compositions of bulk rocks and first-formed phenocrysts as proxies for liquid–crystal equilibrium. This technique is not universally applicable, especially in situations where magma recharge is common, for example, in rocks derived from large ocean-island volcanoes. Eruption of primitive magma in the Cascade arc is not, however, associated with long-lived volcanic centers. Such eruptions are instead typically monogenetic, and the petrology of the magmas is therefore likely to be simpler than in the case where magma repeatedly uses the same conduit. In support of our interpretation, we illustrate below that the first-formed phenocrysts of olivine (Fig. 7), augite, spinel (Fig. 8), and plagioclase (Fig. 9) found in primitive Cascade arc lavas seem to be in equilibrium with their host rocks, with the likely

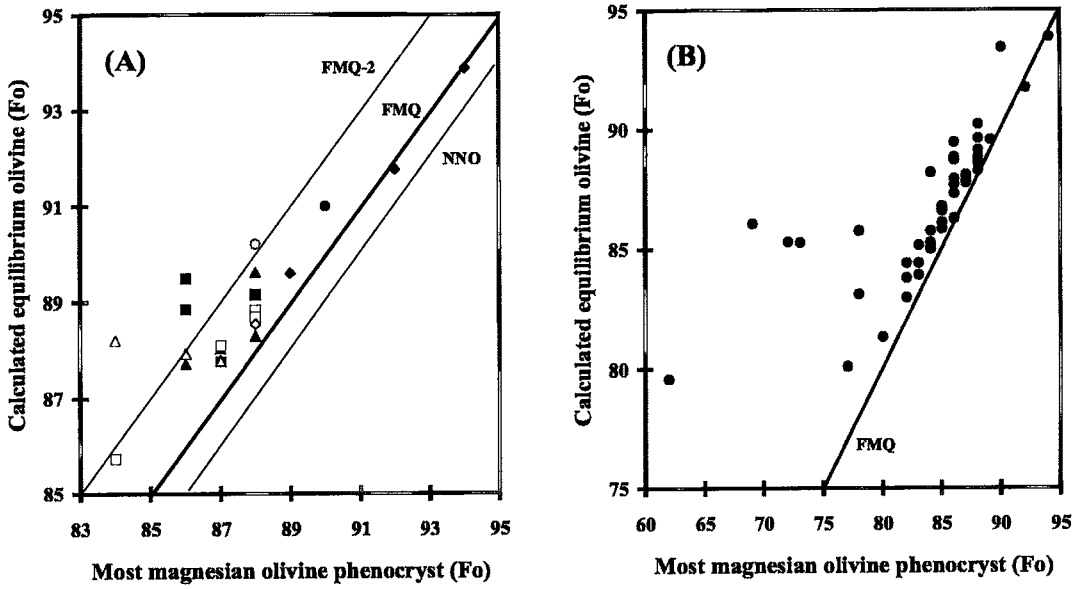

FIG. 7. A. Calculated equilibrium olivine (Roeder & Emslie 1970; K_d = 0.3) *versus* most magnesian phenocrystic olivine in primitive Cascade lavas. All calculations done assuming Fe^{3+}/Fe^{2+} values in bulk rocks consistent with $f(O_2)$ = FMQ (Kress & Carmichael 1991). Lines show approximate range of required equilibrium $f(O_2)$. Note that most bulk-rock compositions could have been in equilibrium with their most magnesian olivine phenocrysts at $f(O_2)$ = FMQ – 2 to NNO. Symbols as in Figure 2. B. Correlation of expected (K_d = 0.3) *versus* observed olivine phenocryst composition in 51 samples of Cascade basalt and basaltic andesite. Samples with olivine less magnesian than Fo_{75} commonly show evidence for resorption of phenocrysts or reaction to form orthopyroxene (or both).

exceptions of amphibole in absarokite and olivine in depleted basaltic andesite.

There is a good correlation between calculated composition of olivine and maximum observed forsterite content in olivine for most samples of Cascade basalt, including primitive basalt (Fig. 7). The few Cascade basalt samples with olivine compositions more Fe-rich than Fo_{75} that do not have apparently near-equilibrium olivine compositions commonly display evidence of reaction (orthopyroxene rim or resorption) between olivine and host. The calculated compositions of olivine assume $f(O_2)$ = FMQ (Kress & Carmichael 1991) and a constant Mg–Fe^{2+} exchange distribution coefficient (K_d) of 0.3 between olivine and bulk rock (Roeder & Emslie 1970). The assumed temperature in each case was calculated using the Roeder and Emslie olivine–liquid geothermometer. The calculated compositions of olivine are insensitive to temperature (a change of 100°C is required to change Fo content by one mol.%) but are sensitive to the values of the exchange K_d and the $f(O_2)$. Raising the K_d value to 0.32 lowers the calculated Fo content of olivine by one mol.%, which would result in a better correspondence between the expected and observed olivine in Cascade basalt. Reducing the oxygen fugacity by one log unit lowers the calculated Fo content of olivine by one mol.% (on average; there is some variation among samples). The most Fo-rich olivine phenocrysts in the majority of Cascade primitive basalt samples therefore have the Fo content expected from their bulk-rock composition if oxygen fugacity was between FMQ – 2 (in log units) and NNO (nickel – nickel oxide oxygen buffer; Fig. 7). The good correlation between expected and observed compositions of olivine is evidence that olivine crystallization was an equilibrium process in Cascade basaltic magmas and that the first-crystallized olivine is preserved in most cases. Reaction between olivine and liquid results in a higher expected Fo content than that actually observed (Fig. 7). Such reaction likely affected the first-formed olivine in some cases, but probably was unimportant overall given the correlation shown in Figure 7.

It is possible that accumulation of olivine has affected the bulk-rock compositions of primitive Cascade rocks and thus rendered the calculated compositions of olivine too Fo-rich. This possibility can be discounted in all but a few cases simply because primitive lavas in the Cascades are so sparsely porphyritic (Table 2). An exception is depleted basaltic andesite, which has an expected olivine composition of Fo_{94} but contains Fo_{90} olivine (maximum). Depleted basaltic andesite is by far the most olivine-phyric of any rock discussed here (Table 2), and the olivine crystals therefore may have been accumulated. Subtraction of

15 weight% olivine and augite (in 4:1 proportions) from the bulk rock yields a composition that could have been in equilibrium with Fo_{91} olivine at an $f(O_2)$ of FMQ – 1. Ample modal olivine is available to do this. If this accumulation is subtracted, the Mg# of the calculated melt is around 76, instead of 81 (Table 1). Early Western Cascade basalt and analcimite, although highly porphyritic, have first-formed phenocrysts that seem to be in equilibrium with their bulk-rock compositions. Therefore, these rocks probably are not cumulates.

The concentrations of Ca and Mn in olivine also suggest equilibrium crystallization. The Ca content of olivine phenocrysts reflects positively the host-rock Ca, in agreement with the relatively constant distribution-coefficient of Ca in olivine in magmas of these compositions at similar temperatures and Fo contents (Jurewicz & Watson 1988, Snyder & Carmichael 1992). The Mn content of olivine increases with decreasing Fo content, as expected, but with the exception of olivine in absarokite (Fig. 6). There is an increase in the K_d for Mn in olivine with increasing K of the host magma (Takahashi 1978), which probably accounts for these high Mn values in absarokite [the K_d for Mn is insensitive to $f(O_2)$: see below, and Snyder & Carmichael (1992)]. The absarokite that shows the lowest increase in the level of Mn in olivine has the lowest K_2O. The K_d must get as large as 4.0, considering the low bulk-rock Mn content in absarokite (Table 1). Other strongly alkaline rocks also have high levels of Mn in olivine (Simkin & Smith 1970).

The compositions of the first-formed (most Mg-rich) spinel closely follow bulk-rock compositions in primitive lavas from the Cascade arc (Fig. 8). The Cr# of spinel is positively correlated with bulk-rock Si/Al (molar) (Dick & Bullen 1984), although the Cascade data define a steeper slope than the data compiled by Dick and Bullen. The Fe3# of spinel follows a simple pattern (Fig. 4), except for spinel in absarokite, implying equilibrium crystallization of most magmas at similar values of $f(O_2)$. The spinel in absarokite seems to have crystallized under more oxidizing conditions, as also suggested by reverse zoning of its olivine (which implies low Fe^{2+} content in the absarokitic magma). The inverse correlation of Cr# and Mg# in spinel (Fig. 4) in primitive lavas from the Cascade arc is similar to the expected trend of equilibrium crystallization of spinel in Fo-rich olivine at high temperature (Roeder 1994). These observations support the interpretation that equilibrium was maintained during crystallization of Cascade primitive magmas.

Pyroxene compositions also seem to reflect equilibrium crystallization. The high Mg# of augite phenocrysts (Fig. 5) is consistent with the high bulk-rock Mg# of these primitive lavas. As expected, the highest Wo contents are found in SiO_2-undersaturated analcimite, and the lowest in the SiO_2-rich depleted basaltic andesite.

Similarly, plagioclase phenocrysts probably were in equilibrium with their host magmas (Fig. 9), although this assessment depends on the $f(H_2O)$ of the host. As

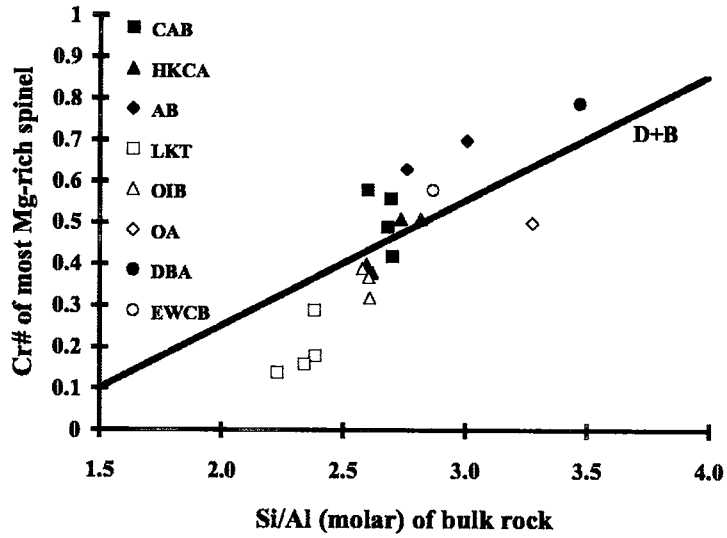

FIG. 8. Spinel Cr# [Cr/(Cr + Al)] *versus* bulk-rock chemistry (Si/Al molar) for primitive Cascade lavas. Only the Cr# values of the highest Mg# spinel in each sample are plotted here. "D + B" line is best-fit line from Dick & Bullen (1984). Cascade data define a steeper slope, especially if the undersaturated OA sample is ignored.

shown below, low-K tholeiites contain the plagioclase compositions expected for dry magma; all other magma contained some H_2O and, hence, more calcic plagioclase than expected in dry systems.

In summary, it seems that first-formed olivine, augite, spinel, and plagioclase phenocrysts in primitive mafic lavas from the Cascade arc crystallized in equilibrium with liquids having the bulk-rock compositions.

Intensive parameters

If equilibrium between first-formed phenocrysts and bulk-rock compositions is assumed, then the intensive variables $f(H_2O)$, $f(O_2)$, T, and P can be evaluated using experimentally established crystal–liquid equilibria. H_2O content can be estimated from changes in phenocryst and groundmass assemblages and with plagioclase–liquid equilibria (Housh & Luhr 1991, Panjasawatwong *et al.* 1995). The presence of olivine and plagioclase phenocrysts in low-K tholeiite, and the correspondence of plagioclase compositions in low-K tholeiite to those expected in dry magma crystallizing at a pressure of 3–5 kbar (Fig. 9), suggest that low-K tholeiitic magmas are nearly anhydrous. Direct measurement of only 0.2 wt% H_2O in glass inclusions in olivine from a low-K tholeiite at Medicine Lake volcano supports this interpretation (Sisson & Layne 1993). The phase relations of a primitive low-K tholeiite from Medicine Lake volcano under anhydrous conditions are consistent with an origin by melting dry spinel peridotite at shallow depths in the mantle (Bartels *et al.* 1991).

Primitive OIB-like basalts, in contrast, are usually only olivine-phyric, in some cases accompanied by plagioclase or augite (Table 2). Plagioclase in OIB-like basalt is consistently too calcic for dry magma crystallizing at 3–5 kbar pressure (Fig. 9), and the groundmass of OIB-like basalt commonly contains traces of phlogopite. These factors suggest that OIB-like magmas contained some H_2O, but commonly were not H_2O-rich at the pressure of phenocryst crystallization (presumed to be 2–5 kbar; see below). Plagioclase would have to be as calcic as An_{90} in OIB-like magmas if they were H_2O-saturated at 2 kbar (Panjasawatwong *et al.* 1995). A much higher H_2O content is likely in analcimite, as indicated by the abundance of phenocryst pyroxene and groundmass biotite. As discussed below, pyroxene phenocrysts in analcimite probably crystallized at shallow pressure (2–5 kbar). The evidence for extensive low-pressure crystallization of pyroxene is consistent with saturation in H_2O (at 2–5 kbar pressure), because saturated magma must degas and crystallize when it reaches shallow depths (Sisson & Grove 1993b).

A progressive increase in H_2O content from nearly anhydrous low-K tholeiite to OIB-like basalt to analcimite is consistent with the relative concentrations of incompatible elements in the rocks, assuming that H_2O also behaves as an incompatible element. The increase in phenocryst content from nearly aphyric low-K tholeiite to porphyritic OIB-like basalt to highly porphyritic analcimite is expected, given such increasing levels of H_2O. The diktytaxitic groundmass texture of low-K tholeiite also implies eruption of nearly anhydrous magma: the absence of substantial eruptive degassing and undercooling should result in low rates of nucleation and high rates of growth during crystallization (Dowty 1980), leading to medium grain-size and a very late concentration of volatiles after crystallization is nearly complete (*i.e.*, a diktytaxitic texture). (Note that low-K tholeiite lava may still be scoriaceous because even magma with 0.2 wt% H_2O is H_2O-saturated at atmospheric pressure. Also, the difference in cooling rates between magma erupted subaerially and

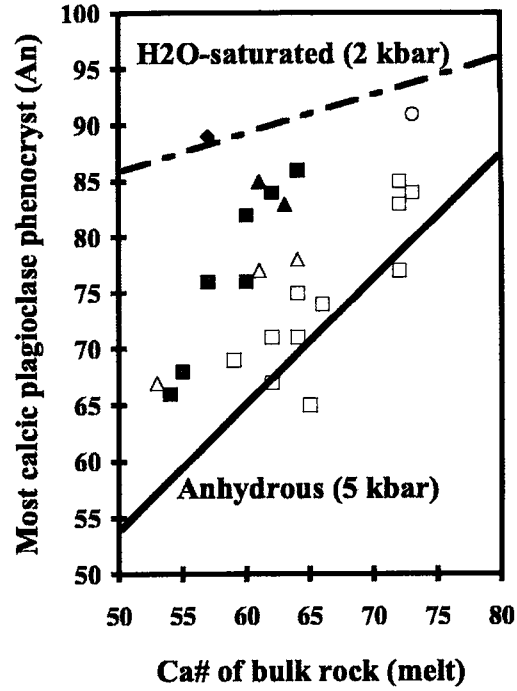

FIG. 9. Most calcic phenocryst of plagioclase (An mol.%) *versus* Ca# [Ca/(Ca + Na) molar] of bulk rock in Cascade basalts and primitive lavas. Symbols as in Figure 2. Unpublished data from samples of more evolved basalt are included here because plagioclase data from primitive samples are sparse. Solid and dashed sloping lines are best fits to anhydrous and H_2O-saturated systems (at 2 kbar), respectively (Panjasawatwong *et al.* 1995). Best fit to plagioclase data for Cascade low-K tholeiite is at 3 kbar anhydrous, not the 5 kbar line shown. Absarokite point is xenocryst derived from disaggregated gabbro in DS90–47; it suggests that absarokitic magmas were H_2O-saturated, or at least that cogenetic gabbro crystallized under H_2O-saturated conditions. Early Western Cascade basalt also seems to have been H_2O-rich. These data suggest OIB-like basaltic, calc-alkaline basaltic, and high-K calc-alkaline basaltic magmas also had substantial H_2O contents.

subaqueously must be kept in mind when considering the textural difference between diktytaxitic Cascade low-K tholeiite and fine-grained or glassy MORB.) The contrasting fine-grained intergranular texture in OIB-like basalt and very fine-grained intergranular texture in analcimite suggest substantial eruptive degassing and undercooling, with consequent high rate of nucleation and low rate of crystal growth.

The series calc-alkaline basalt, high-K calc-alkaline basalt, and absarokite also may be one of increasing H_2O content, although all of these magmas likely contained substantial amounts of H_2O. The increase in incompatible element concentrations from calc-alkaline basalt to high-K calc-alkaline basalt to absarokite is consistent with increasing H_2O content, assuming that H_2O concentrations increase commensurately with the incompatible trace elements. H_2O commonly is considered to be the primary agent of transportation for *LILE* in subduction zones (Stolper & Newman 1994), so a positive correlation of H_2O and *LILE* concentrations in subduction-related rocks might be expected. Phenocryst assemblages change from generally olivine plus plagioclase in calc-alkaline basalt to olivine plus augite in absarokite, consistent with an increase in H_2O content (Yoder 1964, Michael & Chase 1987, Gaetani *et al.* 1993). Relict amphibole is common in absarokite, and virtually absent in other rocks. At 2 kbar pressure, primitive basaltic magmas crystallize amphibole only if nearly H_2O-saturated (Sisson & Grove 1993a). Even if amphibole was not in equilibrium with the host absarokitic magma (its Fe/Mg ratio is too high), its derivation from disaggregated comagmatic hornblende gabbro in absarokite suggests a genetic relationship. The common groundmass phlogopite in calc-alkaline basalt and its increasing abundance in high-K calc-alkaline basalt and absarokite also are consistent with increasing H_2O content (alternatively, this could be ascribed to increasing K concentration accompanied by constant, but substantial, amounts of H_2O). The plagioclase compositions of calc-alkaline basalt and high-K calc-alkaline basalt are consistent with the presence of substantial H_2O, but not with H_2O-saturated crystallization at 2 kbar (Fig. 9; Panjasawatwong *et al.* 1995). The H_2O contents of calc-alkaline basalt suggested by these plagioclase data may be somewhat variable, with a range from perhaps 1 to as much as 2–3 wt%. These numbers are poorly constrained, but are consistent with direct measurements of H_2O content in glass inclusions in Cascade calc-alkaline basaltic andesites from northern California (Anderson 1973, Sisson & Layne 1993). Sparse data on plagioclase in high-K calc-alkaline basalt are consistent with H_2O contents on the high end of the calc-alkaline basalt range (Fig. 9). One sample of absarokite has xenocrystic An_{89} plagioclase, derived from disaggregated hornblende gabbro. Such calcic plagioclase is consistent with crystallization under H_2O-rich conditions (Fig. 9) and the presence of abundant amphibole. The apparent comagmatic nature of the disaggregated hornblende gabbro also is evidence that absarokitic magmas were H_2O-rich. The fine-grained intergranular textures of calc-alkaline basalt, high-K calc-alkaline basalt, and absarokite suggest that substantial eruptive degassing and undercooling occurred in all of these magmas, as in the case of OIB-like basalt and analcimite. Finally, the crude increase in absolute abundance of phenocrysts from calc-alkaline basalt to high-K calc-alkaline basalt to absarokite (Table 2) also is consistent with increasing H_2O content: more H_2O-rich magma undergoes more extensive degassing, and hence crystallizes more completely as it rises to shallow depth (Sisson & Grove 1993b). The presence in absarokite of disaggregated comagmatic gabbros and relics of high-pressure crystallization (pyroxene cores) are expected, given these considerations.

The phenocryst assemblage of primitive depleted basaltic andesite has been duplicated in experiments with similar basaltic andesites from northern California (Baker *et al.* 1994). The California basaltic andesites likely contained from 3 to 5 wt% H_2O at 1150–1200°C and 10 kbar (Baker *et al.* 1994). (No higher pressures were investigated in those experiments, such that the effect of pressure is not well constrained). The sample of depleted basaltic andesite described here probably had similar T and $f(H_2O)$. The highly porphyritic nature of this sample supports the interpretation that this magma was H_2O-rich for the reasons argued above for absarokitic and analcimitic magmas.

Anorthite (An_{91}) found in early Western Cascade basalt is consistent with crystallization under H_2O-saturated conditions at a pressure of 2 kbar or higher (Fig. 9; Panjasawatwong *et al.* 1995). The high phenocryst content and extended range in phenocryst composition in the early Western Cascade basalt sample (Table 2) are also consistent with a high H_2O content: the magma could not have reached shallow pressure without substantial degassing and crystallization (Sisson & Grove 1993b).

Oxygen fugacity was inferred solely from olivine–liquid equilibrium (Roeder & Emslie 1970). As described above, an Fe^{3+}/Fe^{2+} value for each sample was calculated at an assumed $f(O_2)$ equal to FMQ using the expression of Kress and Carmichael (1991) at a temperature given by the Roeder & Emslie olivine–liquid thermometer. (Some iteration was required to equalize the temperature in both expressions). As noted above, variations in $f(O_2)$ have a significant effect on olivine composition: changing the $f(O_2)$ by one log unit typically changes the expected olivine composition by one mol.% Fo (Fig. 7). Most of the rocks examined (including an "unaccumulated" depleted basaltic andesite) could have been in equilibrium with their most Mg-rich olivine phenocrysts at an $f(O_2)$ between FMQ – 2 and NNO (Fig. 7). Absarokitic magma seems to be systematically more oxidized than other magma, but the difference is only 1–2 log units. Calculation of $f(O_2)$ values from olivine–liquid equilibria for these samples by

Kevin Richter (pers. comm. 1996) yields similar results to those shown in Figure 7, but with one important exception. Kevin's method of calculation is similar to the one employed here, but he allows K_d values to vary depending on composition. Compositional variations have little effect on the K_d for most magmas except for those of absarokitic character. They appear to be more strongly oxidized (FMQ + 2 to FMQ + 3) than indicated by the results shown in Figure 7. There are also some indications in the new calculations that OIB-like basalt is somewhat less oxidized (FMQ – 2) than low-K tholeiite and calk-alkaline and high-K calk-alkaline basalt (FMQ).

The more oxidized character of absarokitic magma is reflected also in the reverse zoning of its olivine (Fig. 6) and higher calculated Fe^{3+} in spinel (Fig. 4). These inferences are in agreement with $f(O_2)$ values estimated for mantle xenolith suites, where the range in $f(O_2)$ is from FMQ – 2 to FMQ + 2, and the more oxidized xenoliths are considered to have been influenced by subduction (Mattioli *et al.* 1989, Wood *et al.* 1990). Reports of much higher values of $f(O_2)$ (to FMQ + 5) in subduction-related rocks in western Mexico (Carmichael 1991) are not based on the method used here and are inconsistent with olivine– liquid equilibrium (*cf.* Righter *et al.* 1995, Table 5).

Liquidus temperatures can be evaluated with olivine–liquid or olivine–liquid–H_2O thermometry (Roeder & Emslie 1970, Sisson & Grove 1993b). Calculated liquidus temperatures for low-K tholeiite were found to be consistent using both geothermometers (assuming no H_2O present and 3 kbar pressure, as suggested by plagioclase compositions). The two southernmost low-K tholeiite samples yield 1215–1240°C, the two RCBD-prefixed samples give 1230–1250°C, and the northernmost sample, 1240–1260°C. If these results are meaningful, they suggest the temperature of low-K tholeiitic magma increased northward as eruption rates and degree of melting declined (see below). As argued below, the northernmost low-K tholeiite had a deeper origin at lower degrees of partial melting than the southernmost low-K tholeiite, an interpretation consistent with these temperature data: deeper, lower-degree melts of peridotite should be hotter than shallow, higher-degree melts due to the increase in the heat of fusion of basaltic magma with pressure (Fukuyama 1985). Assuming a rate of adiabatic cooling during magma ascent of 1°C/km (McKenzie & Bickle 1988), southern low-K tholeiite could have been generated by partial melting of peridotite at approximately 1280°C at an average depth of 50 km (*cf.* Bartels *et al.* 1991), whereas northern low-K tholeiite may have been formed at an average depth of 70 km at around 1320°C. The high Fe content of northern low-K tholeiite is consistent with such an interpretation because more Fe partitions into melt at higher temperature (Roeder & Emslie 1970, Gaetani & Grove 1995).

Similar calculations for OIB-like basalt yield the same result: the northernmost OIB-like basalt gives 20–30°C higher temperatures than the two southern ones using these thermometers (using the same assumptions as for low-K tholeiite). The same arguments applied to low-K tholeiite also apply to OIB-like basalt (see below): the degree of melting is probably lower in the north, and melting occurs at deeper levels. The calculated temperatures are similar to those found for low-K tholeiite: 1210–1240°C for southern OIB-like basalt, and 1240–1260°C for northern occurrences. These are calculated for the dry case, so would be about 20°C too high if 1% H_2O were present (Sisson & Grove 1993b).

Estimation of liquidus temperatures for the H_2O-bearing, subduction-related basalts requires knowledge of H_2O concentrations, because the presence of H_2O lowers liquidus temperatures (Sisson & Grove 1993b). The most suitable geothermometer for these basalts is that calibrated by Sisson & Grove (1993b) because it takes into account the effects of H_2O content as well as pressure of crystallization. If a constant H_2O content of 3 wt% is assumed (and a pressure of 3 kbar), calculated liquidus temperatures decline in the order calc-alkaline basalt, high-K calc-alkaline basalt, absarokite, from 1130–1170°C to 1110–1160°C to 1105–1145°C, respectively. Because of the evidence for an increase in H_2O content in the same series, this decline in liquidus temperature is probably real and more pronounced than presumed here. The absolute temperatures cannot be predicted better without more knowledge of H_2O content.

An estimate of H_2O content and liquidus temperature can be made for absarokite sample DS90–47 on the basis of simultaneous solution of the olivine–liquid–H_2O (Sisson & Grove 1993b) and plagioclase–liquid–H_2O (Housh & Luhr 1991) geothermometers. Assuming H_2O saturation at 3 kbar and An_{89} as the equilibrium plagioclase, the best fit to both thermohygrometers is found at 4 wt% H_2O and 1080°C (using only the An equation of the Housh & Luhr formula, as recommended by Sisson & Grove). Similar calculations for calc-alkaline basalt and high-K calc-alkaline basalt can be used to infer H_2O content and liquidus temperature; however, a plagioclase composition needs to be assumed for these calculations, because many of the primitive samples lack plagioclase phenocrysts. If an average plagioclase composition of An_{80} is assumed for calc-alkaline basalt (Fig. 9), and one of An_{85} for high-K calc-alkaline basalt and absarokite, average calculated temperatures decline in the order calc-alkaline basalt, high-K calc-alkaline basalt, absarokite from 1145° to 1135° to 1120°C, respectively. Calculated H_2O content rises in the same series from 3.0 to 3.25 to 3.5 wt% on average.

A similar calculation was undertaken for early Western Cascade basalt assuming a pressure of 3 kbar and An_{91} equilibrium plagioclase. The best fit to both geothermometers is found at 2% H_2O and 1200°C. Olivine–liquid–H_2O thermometry (Sisson & Grove 1993b) gives a calculated temperature of 1150°C with

4% H_2O at 3 kbar for depleted basaltic andesite, similar to the range of conditions estimated experimentally for primitive basaltic andesite in northern California (Baker *et al.* 1994). Analcimite gives 1170°C with 3% H_2O.

The pressure of phenocryst crystallization can be roughly estimated by considering phenocryst assemblages and compositions. The presence of olivine plus plagioclase in many of the lavas suggests that crystallization occurred within the crust (≤8 kbar). Plagioclase compositions in low-K tholeiite are those expected at 3 kbar on average (Fig. 9). The low Al and Na concentrations in pyroxene phenocrysts in analcimite, high-K calc-alkaline basalt, absarokite, early Western Cascade basalt, and depleted basaltic andesite suggest crystallization at low to modest (≤8 kbar) pressures. More Fe-rich relict cores in augite in absarokite probably crystallized at higher pressure, as inferred from their high Na and ^{VI}Al contents (approx. 0.06 and 0.10 *apfu*, respectively). Mg-rich augite overgrown on these cores is richer in Na and ^{VI}Al than in the case where such cores are lacking. The high-pressure relics seem to have served as nuclei for "earlier than usual" growth of pyroxene phenocrysts. The evidence that most crystallization occurred at shallow depths is consistent with the rise of virtually aphyric magma to crustal levels, where it encounters saturation limits and is forced to crystallize (Sisson & Grove 1993b). The degree to which the magmas crystallize depends on H_2O content: those with more H_2O crystallize more extensively, and crystallization begins at greater depth. The presence of high-pressure relict pyroxene in the most H_2O-rich absarokitic magmas, and the absence of such relics in other magma, are thus expected because absarokitic magma reaches H_2O-saturation at the highest pressure.

Degree and depth of partial melting

Primitive magmas erupted in the northern Oregon and southern Washington Cascades over the last 8 million years are closely related to the propagation of an intra-arc rift (Fig. 1). Higher degrees of partial melting associated with rifting led to the eruption of low-K tholeiite (Conrey *et al.* 1994). The highest degrees of melting, based on Na_2O–MgO relations, were reached beneath the southern end of the rift in central Oregon. Low-K tholeiite in northernmost Oregon and southern Washington was derived by lower degrees of melting. Post-rift (and syn-rift on the northernmost end of the rift) eruptions have involved lower degrees of melting, yielding a spectrum of OIB-like basalt, calc-alkaline basalt, high-K calc-alkaline basalt, and absarokite. Of these, high-K calc-alkaline basalt and absarokite appear only where the degree of melting is very small (and eruption rates are lowest: Sherrod & Smith 1990). These field-based and geochemical interpretations are the basis for the following discussion.

Dry melting of spinel or plagioclase peridotite is fairly well understood (see references in Introduction), and the major-element composition of low-K tholeiite is consistent with experimental data. For example, the high Al (~17.5 wt% Al_2O_3) and Ca (~11.5 wt% CaO) and low FeO* (~9.0 wt%) contents of southern primitive low-K tholeiite are consistent with an origin by 20–30% partial melting of dry spinel peridotite at 15 kbar (Hirose & Kushiro 1993). In contrast, the lower Al (~16.7 wt% Al_2O_3) and Ca (~9.5 wt% CaO), and higher FeO* (~11.5 wt%) contents of the northernmost low-K tholeiite are consistent with an origin involving 10% or less partial melting of dry peridotite at 25 kbar (Hirose & Kushiro 1993). These data agree with the Na_2O–MgO relationships noted above: southern low-K tholeiite has lower Na_2O concentrations at a given MgO content than northern occurrences (Conrey *et al.* 1994). Northern low-K tholeiite cannot be derived from the same depth as the southern occurrences because FeO* is smaller at lower degrees of partial melting at constant pressure. This would require northern low-K tholeiite to be derived by higher degrees of partial melting, inconsistent with the Na_2O, CaO, and Al_2O_3 data.

Trace-element data strengthen this interpretation; for example, chondrite-normalized Ce/Yb values are higher, and Y/Zr and Sc values are lower in northern low-K tholeiite (Table 1, Fig. 10). These trace-element ratios and Sc are depth-sensitive because Sc and Yb are highly compatible in garnet. Dynamic melting models (where melts are pooled from a range of depths in a melt column) of peridotite suggest that Ce/Yb values are higher and Y/Zr values are lower as the average depth of melt extraction increases (McKenzie & O'Nions 1991, Elliot *et al.* 1991, Eggins 1992, Devey *et al.* 1994, Shen & Forsyth 1995). If these models and interpretations are correct, the average depth of generation for southern low-K tholeiite was in the spinel lherzolite field of stability, whereas that for northern low-K tholeiite was substantially deeper, probably on or near the boundary of the garnet and spinel lherzolite fields.

The trace-element pattern of low-K tholeiite is not identical to typical MORB (Fig. 3), raising the question of whether subduction has metasomatized its mantle source. Addition of only 3–4% absarokite to average MORB can produce the trace-element pattern of low-K tholeiite; however, the presence of rare reversely zoned intermediate plagioclase xenocrysts (Table 2) suggests that some crustal assimilation has occurred as well. The trace-element pattern of low-K tholeiite suggests a lithospheric source, probably contaminated by subduction. A lithospheric origin also is supported by the regional isotopic variation of low-K tholeiite, which follows that of the overlying crust (Hart 1985, Bacon *et al.* 1996, Gunn *et al.* 1996).

The same contrast in major elements found in low-K tholeiite is seen in OIB-like basalt: the northernmost OIB-like basalt has lower SiO_2, Al_2O_3, and CaO, and higher FeO* than the southern occurrences (Table 1). These data suggest a deeper origin for the northern

OIB-like basalt. Some trace-element data support this interpretation, as the northern OIB-like basalt has lower Sc than the southern, but *REE* data are lacking. Compared to low-K tholeiite, OIB-like basalt has higher Na, Nb, Nb/Zr, and lower Sc and Y/Zr (Table 1, Fig. 10), all consistent with a lower degree of partial melting at deeper average levels (asthenospheric), where garnet is a residual phase. Melting models of the same mantle cannot reproduce the spectrum of trace-element abundances in low-K tholeiite and OIB-like basalt (Fig. 10): the OIB-like basalt source-mantle must be more enriched in Nb and other incompatible trace-elements than low-K tholeiite source-mantle. OIB-like basalt also is consistently slightly more radiogenic in Sr and Pb, and less radiogenic in Nd, than low-K tholeiite (Gunn *et al.* 1996), consistent with its derivation from deeper, less depleted mantle (*cf.* Elliot *et al.* 1991). Dry melting experiments of peridotite broadly agree with the interpretation that OIB-like basalt forms by low (≤5%) degrees of partial melting at 20–30 kbar (Hirose & Kushiro 1993); however, the experiments do not extend to the low degrees of melting likely for the generation of the Cascade OIB-like basalt (probably ≤2–5%), such that it is not possible to fully interpret their major-element composition. The evidence for the presence of up to 1% H_2O in OIB-like basalt magmas (see above) suggests a possible role for a hydrous phase, presumably fluor-pargasite, during low degrees of partial melting (Foley 1991).

Analcimite does not correspond to a partial melt of dry peridotite because the Ca content is too high (~13 wt% CaO), and Al too low (~11 wt% Al_2O_3) to be consistent with its low SiO_2 and high FeO*. The low SiO_2 and high FeO* suggest high-pressure melting, but dry low-degree partial melts at 20–30 kbar should have low CaO and higher Al_2O_3 (Hirose & Kushiro 1993). This suggests the presence of a hydrous phase, likely amphibole, that controls the major elements during very low degrees of partial melting [see further arguments in Conrey (1990)]. The trace-element patterns in analcimite suggest melting in the garnet lherzolite depth range (Fig. 10). Alternatively, analcimitic magma may be produced by remelting non-peridotite (amphibolite, or possibly pyroxenite) metasomatic veins emplaced into lower-pressure spinel lherzolite (Conrey 1990). Analcimitic magma is similar to the metasomatic agent inferred to transport volatiles and incompatible elements, and to form amphibole-rich dikes in within-plate mantle (Hawkesworth *et al.* 1984). One possible interpretation is that the enrichment of OIB-like basalt source-mantle in Nb and other incompatible elements (Fig. 10) is due to metasomatism by analcimitic magma.

The major-element compositions of the subduction-related primitive basalts also are inexplicable in terms of dry peridotite melting. Recent experiments on wet melting of peridotite demonstrate that H_2O strongly influences melt composition (Gaetani & Grove 1995). The main effect of H_2O is to lower FeO* in the melt due to an increase in the Fe bulk distribution-coefficient with lower temperature (H_2O also lowers the liquidus temperature). These experiments are consistent with the generally low FeO* contents of calc-alkaline basalt, high-K calc-alkaline basalt, absarokite, depleted basaltic andesite, and early Western Cascade basalt. However, FeO* content ranges widely in primitive calc-alkaline basalt (and in these subduction-related basalts as a whole: see Table 1), in agreement with the suggestion from plagioclase–liquid relations that calc-alkaline basalts (and other subduction-related basalts) have variable H_2O contents (Fig. 9). Absarokite has the most uniform composition among the subduction-related basalts, with a range in FeO* from 6.8 to 8.3 wt%. If melt FeO* varies directly with temperature at the same pressure, then the consistently lower FeO* in absarokite agrees with the temperature estimates discussed above: that is, absarokite had a lower liquidus temperature than high-K calc-alkaline basalt, which in turn had a lower temperature than calc-alkaline basalt, if we assume that all of these magmas were generated at about the same depth.

Trace-element and isotopic data bear on the question of average depth of generation of calc-alkaline basalt and high-K calc-alkaline basalt. The Ce/Yb and Y/Zr values of calc-alkaline basalt and high-K calc-alkaline basalt overlap the range in ratios found in OIB-like basalt and analcimite (Fig. 10). These ratios suggest similar average depths of melt generation in the garnet lherzolite field. The range in Sc concentrations in primitive calc-alkaline basalt and high-K calc-alkaline basalt (20–33 ppm) is also similar to that in OIB-like basalt (26–31 ppm). Nd and Pb isotope ratios of primitive calc-alkaline basalt and high-K calc-alkaline basalt overlap those of OIB-like basalt, whereas Sr is consistently slightly more radiogenic in the subduction-related basalts (Gunn *et al.* 1996). These data are consistent with a model in which calc-alkaline basaltic and high-K calc-alkaline basaltic magmas were generated from similar or slightly greater depths than OIB-like basaltic magmas, except that the former magmas were derived from parcels of subduction-modified mantle.

Absarokite has the lowest Sc content and Y/Zr values and the highest Ce/Yb values (Fig. 10), suggesting that residual garnet was of greatest abundance in its source region, perhaps in the deepest levels of the melt column. The high Ce/Yb values could result from a process combining the effects of garnet in both the mantle wedge and the subducted slab. Slab involvement in absarokite genesis is consistent with isotopic data: absarokite has Nd and Pb isotope ratios similar to those in calc-alkaline basalt and high-K calc-alkaline basalt, but absarokitic samples have the most radiogenic Sr in the Cascades. The radiogenic Sr can be explained by mixing ≤0.5% subducted pelagic sediment into the mantle wedge (Gunn *et al.* 1996).

A role for the slab also is suggested by the low concentrations of Nb in absarokite (Fig. 10). The rarity and small erupted volume of absarokite suggest that it

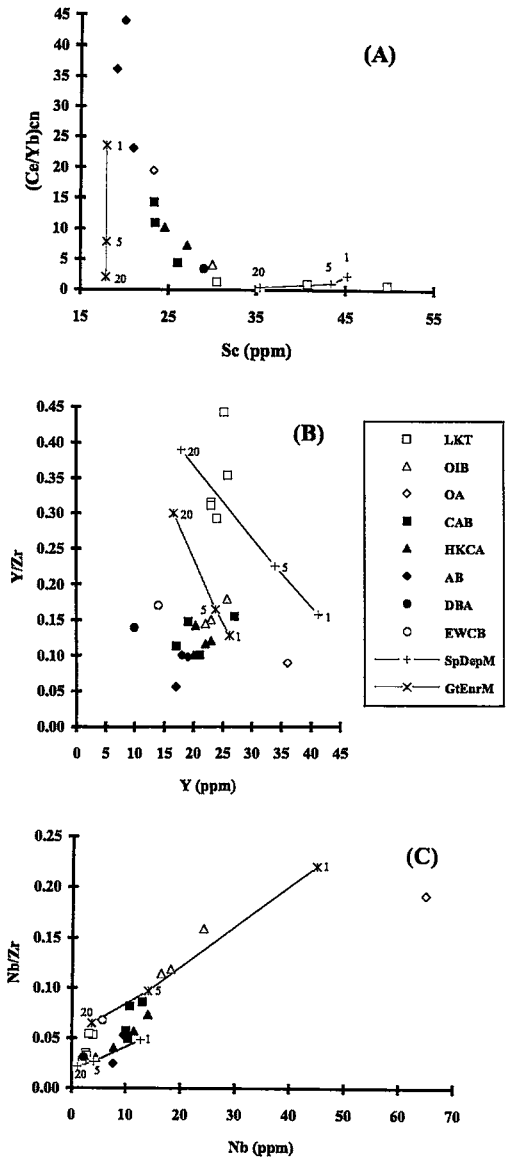

FIG. 10. Chemical data critical in evaluating average depth and degree of partial melting during generation of primitive magmas in the Cascade arc. A) Chondrite-normalized Ce/Yb *versus* Sc (ppm). B) Y/Zr *versus* Y (ppm). Southern low-K tholeiite has Y/Zr ≥ 0.35, whereas in northern low-K tholeiite, it is approximately 0.30. C) Nb/Zr *versus* Nb (ppm). All plots show aggregated fractional melt models (Shaw 1970) for reference (symbols at 1, 5, and 20% aggregate melting). "SpDepM" (spinel lherzolite depleted mantle) model derived using "fertile MORB mantle" data and 1300°C bulk partition-coefficients of Pearce & Parkinson (1993), with Ce data from McKenzie & O'Nions (1991). "GtEnrM" (garnet lherzolite enriched mantle) model similarly derived using "primitive undepleted mantle" of Pearce & Parkinson (1993), with Ce data from McKenzie & O'Nions (1991). These models approximate more realistic dynamic melting models as long as most melting occurs at either shallow depths in depleted mantle (SpDepM) or in deeper, less depleted mantle (GtEnrM). The models are consistent with the assertion that low-K tholeiite represents higher degrees of melting of shallow, depleted mantle, whereas OIB-like basalt, calc-alkaline basalt, high-K calc-alkaline basalt, and absarokite represent lower degrees of melting of less depleted mantle. Note that the low Sc in absarokite requires the participation of garnet.

represents the lowest degree of partial melting. Therefore, absarokite should have higher Nb on average than calc-alkaline basalt or high-K calc-alkaline basalt. The reverse is true: primitive calc-alkaline basalt has higher average Nb than high-K calc-alkaline basalt, which in turn has higher Nb than absarokite (Table 1, Fig. 10). This requires that either the absarokite source-mantle is more depleted in Nb, or Nb is retained during generation of absarokitic magma. It is unlikely that a Nb-rich mineral is residual during peridotite melting (Green & Pearson 1986, Ryerson & Watson 1987), but it is possible that either 1) Nb has been retained in the slab during expulsion of a fluid or silicic melt (references quoted above), 2) Nb has been depleted in the vicinity of the slab by previous extraction of melt (Woodhead *et al.* 1993, Hochstaedter *et al.* 1996), or even that 3) Nb has been flushed from the immediate mantle-volume near the slab by an aqueous fluid (Ayers & Watson 1993). Another possibility is that Nb is depleted in absarokitic magma by reaction with peridotite (Kelemen *et al.* 1993); the magnitude of the Nb depletion in absarokite agrees roughly with the depletions produced

by peridotite-assimilation models. Such assimilation is considered to be more likely for small-degree hydrous melts than larger-degree anhydrous melts (Kelemen *et al.* 1990), such that the decrease in Nb concentrations from calc-alkaline basalt to high-K calc-alkaline basalt to absarokite agrees with such a model, as the hydrous small-degree absarokitic melts would react more than the progressively less hydrous high-K calc-alkaline basaltic and calc-alkaline basaltic melts. These melt-reaction models are suspect, however, because the end product of such reaction is a high-Mg andesite (Kelemen *et al.* 1993). If this style of reaction has affected the absarokitic magmas, it has not resulted in high-Mg andesite; in fact, the more SiO_2-rich calc-alkaline basalt and high-K calc-alkaline basalt tend to have higher, not lower, Nb contents (Table 1). A further possibility is that absarokite represents melting of metasomatic veins intruded at shallow depths (similar to the possible interpretation for analcimite). Absarokitic magma may be generated by melting phlogopite-bearing peridotite (argued below), but it is impossible to pick among these competing hypotheses in the absence of a better understanding of melting relations in wet peridotite and the manner in which melts are generated and ascend in the mantle wedge.

The trace-element character of early Western Cascade basalt is unlike that of any of the modern Cascade basalts (Figs. 3, 10). The low Nb and Nb/Zr (and probably Ce/Yb) and high Sc values (Table 1) are low-K-tholeiite-like, but the low Y and Y/Zr values are more calc-alkaline-basalt-like. These combinations suggest contributions from a wide range of depths in a dynamic melt-column. The role of deeper, garnet-influenced melting is perhaps seen in the low Y and Y/Zr values, whereas extensive melting at shallower depths is required to produce the high Sc and low Nb concentrations. This combination is more "arc-like" in that early Western Cascade basalt more closely resembles primitive arc basalt from arcs, where volcanism and partial melting are more vigorous than in the young Cascades.

It is difficult to place depleted basaltic andesite in a partial melt model. The field evidence (age, location, and small erupted volume) suggests that this primitive basaltic andesite represents a low-degree melt of mantle beneath the frontal portion of the arc due to thermal perturbation caused by intra-arc rifting. However, a low degree of partial melting is consistent with the trace-element concentrations in depleted basaltic andesite only if the source is depleted. For example, the low Nb and Nb/Zr values of depleted basaltic andesite are similar to those in low-K tholeiite (Fig. 10). Low Y, Y/Zr, relatively low Sc and relatively high Ce/Yb values all suggest the influence of garnet. The best source for depleted basaltic andesite may be depleted harzburgite, possibly below the depth where garnet is stabilized. The other alternative is to have the depleted basaltic andesite source be shallower, with the trace-element budget controlled either by 1) depletion during prior melting events, with subsequent subduction-related enrichment of selected elements, or by 2) reaction-assimilation (Kelemen *et al.* 1993). The interpretation that similar primitive basaltic andesite in northern California was produced by 20–30% partial melting (Baker *et al.* 1994) is inconsistent with the low abundance and erupted volume of such lavas. The depleted basaltic andesite source may indeed have undergone 20–30% melting (and produced early Western Cascade basalt?), but that must have occurred before it was remelted to form the depleted basaltic andesite.

Model of Cascade subduction

The intensive parameters inferred in this study can be used to constrain models of Cascade subduction. The overall low degree of post-7-Ma partial melting, apart from intra-arc rifting, has allowed deep, low-degree melts to reach the surface. These melts are not commonly seen in arcs, presumably because of dilution in the melt column by higher-degree melts at shallower depth. Cascade absarokite appears to have been generated closer to the subducted slab than other mantle-derived magmas. It is too mafic to be a direct slab-derived melt, but it may be a slab-derived melt that has reacted extensively with peridotite. If an adiabatic cooling during ascent of absarokitic magma of 1°C/km is assumed, the temperature of partial melting of absarokite source-mantle would have been about 1200°C at a depth of 100 km. This modest temperature and the high inferred H_2O content (~4%) of absarokitic magma are consistent with the interpretation that relatively cool, wet (and mildly oxidized) melts rise from the region of the slab to metasomatize the overlying mantle-wedge (*cf.* Yogodzinski *et al.* 1995). If the inferences derived herein concerning intensive parameters are correct, the mantle wedge is cooler closer to the slab; recall that the estimated temperature of partial melting of low-K tholeiite source-mantle is 1280–1320°C at a depth of 50–70 km. Inverted thermal profiles are produced in numerical models of subduction because the slab is cooler than the surrounding mantle (Hsui & Toksöz 1979).

Melting of the variably contaminated wedge could yield hotter and drier (and less oxidized) high-K calc-alkaline basalt and calc-alkaline basalt. Pristine parts of the wedge could melt at low degrees to form OIB-like basalt at deep levels, or, with more melting, extend the melt column up into the spinel lherzolite field to produce low-K tholeiite. The difference between OIB-like basalt and low-K tholeiite seems to reflect melting of deeper, uncontaminated, asthenospheric mantle *versus* melting of shallow, subduction-modified lithospheric mantle. The absarokite – high-K calc-alkaline basalt – calc-alkaline basalt spectrum in the Cascades is similar to the spectrum of shoshonitic – island-arc tholeiitic magmas found in many arcs (*e.g.*, Gill & Whelan 1989,

Lin *et al.* 1989, Rogers & Setterfield 1994). The difference is primarily in the degree and depth of partial melting. The Cascade system is weak (slowly subducting young crust) and, consequently, only deep, low-degree melts are generated. In contrast, vigorous (rapid subduction of older, altered crust) intra-oceanic arc systems establish (hydrated) melt columns that extend upward to shallow levels, where large degrees of melting occur. The difference can be seen in the trace-element abundances: typical arc shoshonites have much lower $(Ce/Yb)_{cn}$ ($\leq$10) and Sr ($\leq$1800 ppm; commonly $\leq$900 ppm) than Cascade absarokite (references noted above). Typical island-arc tholeiites have low Ce/Yb values and are highly depleted in Nb (Pearce & Parkinson 1993; other references in Introduction), whereas Cascade calc-alkaline basalt are not. These differences probably reflect mainly garnet lherzolite melting beneath the Cascades *versus* mainly spinel lherzolite melting beneath most arcs.

The high K content of absarokite suggests an origin *via* partial melting of phlogopite peridotite. Solidus temperatures of phlogopite peridotite range from 1000° to 1175°C at 20–30 kbar (Bravo & O'Hara 1975, Wendlandt & Eggler 1980, Thibault *et al.* 1992, Sekine & Wyllie 1982); the temperature of partial melting estimated for Cascade absarokite falls on the high end of this range. Phlogopite is believed to form in the mantle wedge owing to either fluid- or melt-dominated subduction-zone metasomatism (Sekine & Wyllie 1982, Sudo & Tatsumi 1990, McInnes & Cameron 1994). Common hydrous metasomatism in the mantle, found in mantle-derived xenoliths, has features that suggest a relation to subduction (Hawkesworth *et al.* 1984): 1) a narrow compositional range in metasomatic, low-Ti, H_2O-rich phlogopite (Menzies *et al.* 1987), and 2) a decrease upward (*e.g.*, in the mantle wedge) in K/Na ratio of metasomatic minerals (Arai 1986) similar to the progression from absarokite to high-K calc-alkaline basalt to calc-alkaline basalt. The relative constancy of absarokite compositions is consistent with melting a relatively uniform phlogopite-bearing source. A decrease upward in K (and other *LILE*) away from the subducted slab is expected if the slab is the source of the metasomatizing agent.

The early Western Cascade subduction system must have been a vigorous one, as seen both in the petrology of early Western Cascade basalt and in high rates of eruption and subduction (Verplanck & Duncan 1987). Early Western Cascade basalt appears to have been H_2O-saturated and was derived by a considerably higher degree of partial melting than younger calc-alkaline basalt. The degree of partial melting was likely similar to that for younger low-K tholeiite, and occurred primarily in the shallow part of the spinel lherzolite field of stability, judging from the Nb and Sc concentrations (Table 1, Fig. 10). A strong subduction-induced influence is indicated, however, with low Y and Y/Zr values both suggesting the importance of deep, garnet-influenced melts. The contrast with younger low-K tholeiite is notable in this light: the (passive?) mantle upwelling during rifting that gave rise to low-K tholeiite clearly melted different mantle and in a different way than the mantle that yielded early Western Cascade basalt.

The presence of sparse primitive basaltic andesites in the trenchward part of the arc during intra-arc rifting, and their subduction-influenced composition, offer further clues into the sub-Cascade mantle structure. Depleted basaltic andesite was probably derived from depleted harzburgite that formed during earlier high-degree melting events, possibly the ones that gave rise to early Western Cascade basalt. The genesis of similar high-Mg andesite is still disputed, however. Most hypotheses invoke harzburgite in some form, but there is no agreement whether harzburgite is melted directly (Tatsumi 1981, Umino & Kushiro 1989) or assimilated by other melts (Fisk 1986, Kelemen *et al.* 1993, Yogodzinski *et al.* 1994). The Cascade depleted basaltic andesite suggests that at least some part of the arc front is underlain by harzburgite, which melts under H_2O-rich conditions only when extra heat is supplied during intra-arc rifting (Tatsumi & Maruyama 1989). Melt models suggest that melting takes place in the presence of garnet (Fig. 10), implying a depth near that of the subducted slab (~70–80 km).

Conclusions

We have presented nearly complete petrological data on a suite of primitive rocks from the Cascade arc, and interpreted those data in terms of intensive parameters of the original magmas. The intensive parameters are the first-order guide to any petrogenetic model of the thermal and fluid regime established during subduction. Our primary conclusions are as follows:

1) A diverse suite of primitive magmas has erupted in the Cascades in the past 7 m.y. The petrological diversity requires a complicated, heterogeneous mantle.

2) Subduction processes have had little, if any, effect on the uppermost, lithospheric, spinel-bearing mantle beneath the Cascades during the past 7 m.y. Nearly anhydrous low-K tholeiitic magmas, with MORB-like composition, have resulted from upwelling and decompression-induced melting of that mantle. Some deeper, less depleted, garnet-bearing asthenospheric mantle has also been little affected by subduction, and has melted to produce OIB-like magmas.

3) Subduction has metasomatized the deeper, garnet-bearing parts of the sub-Cascade mantle during the past 7 m.y., producing a wide spectrum of wet calc-alkaline magmas by low degrees of partial melting. The coolest, wettest, and deepest of these magmas are probably derived from metasomatized phlogopite peridotite directly above the subducted slab. These magmas may serve as the metasomatizing agent that transports *LILE* into other parts of the mantle wedge. Alternatively, they may be derived by interaction of (silicic) slab-related

melts or fluids with peridotite, and those melts or fluids are the metasomatizing agents.

4) The early history of the Cascade arc was characterized by more vigorous subduction and a more extensive and dynamic melt-column that extended up into the shallow field of spinel lherzolite. The degree of partial melting was much higher than in the past 7 m.y., and the magmas were probably H_2O-rich.

5) Primitive depleted basaltic andesite was erupted in the frontal arc region in northern Oregon during intra-arc rifting. This magma was probably H_2O-rich and derived from low-degree partial melting of depleted garnet harzburgite.

ACKNOWLEDGEMENTS

Part of the data was collected while Conrey was a post-doctoral fellow at the GSJ. He thanks Kozo Uto, Shigeko Togashi, Hikari Kamioka, and Laureen C. Wagoner for assistance with XRF and INA analyses. Scott Cornelius, Diane Johnson, and Charles Knaack cheerfully and expertly operated and maintained the WSU Geoanalytical Lab. Marv Beeson and Terry Tolan at Portland State University provided sample 92TB16. We thank Graham Nixon and Dana Johnston for organizing an excellent symposium and encouraging this publication. The comments of reviewers Tom Sisson and Dennis Geist resulted in substantial improvements to the manuscript. Robert Martin's thorough editing was much appreciated.

REFERENCES

ANDERSON, A.T. (1973): The before-eruption water content of some high-alumina magmas. *Bull. Volcanol.* **37**, 530-552.

ARAI, S. (1986): K/Na variation in phlogopite and amphibole of upper mantle peridotites due to fractionation of the metasomatizing fluids. *J. Geol.* **94**, 436-444.

ARCULUS, R.J. & POWELL, R. (1986): Source component mixing in the regions of arc magma generation. *J. Geophys. Res.* **91**, 5913-5926.

AYERS, J.C. & WATSON, E.B. (1993): Rutile solubility and mobility in supercritical aqueous fluids. *Contrib. Mineral. Petrol.* **114**, 321-330.

BACON, C.R. (1990): Calc-alkaline, shoshonitic, and primitive tholeiitic lavas from monogenetic volcanoes near Crater Lake, Oregon. *J. Petrol.* **31**, 135-166.

_____, BRUGGMAN, P.E., CHRISTIANSEN, R.L., CLYNNE, M.A., DONNELLY-NOLAN, J.M. & HILDRETH, W. (1997): Primitive magmas at five Cascade volcanic fields: melts from hot, heterogeneous sub-arc mantle. *Can. Mineral.* **35**, 397-424.

BAILEY, D.G. & CONREY, R.M. (1992): Common parent magma for Miocene to Holocene mafic volcanism in the northwestern United States. *Geology* **20**, 1131-1134.

BAKER, M.B., GROVE, T.L., KINZLER, R.J., DONNELLY-NOLAN, J.M. & WANDLESS, G.A. (1991): Origin of compositional zonation (high-alumina basalt to basaltic andesite) in the Giant Crater lava field, Medicine Lake volcano, northern California. *J. Geophys. Res.* **96**, 21819-21842.

_____, _____ & PRICE, R. (1994): Primitive basalts and andesites from the Mt. Shasta region, N. California: products of varying melt fraction and water content. *Contrib. Mineral. Petrol.* **118**, 111-129.

BARTELS, K.S., KINZLER, R.J. & GROVE, T.L. (1991): High pressure phase relations of primitive high-alumina basalts from Medicine Lake volcano, northern California. *Contrib. Mineral. Petrol.* **108**, 253-270.

BRAVO, M.S. & O'HARA, M.J. (1975): Partial melting of phlogopite-bearing synthetic spinel- and garnet-lherzolites. *Phys. Chem. Earth* **9**, 845-854.

CARMICHAEL, I.S.E. (1991): The redox states of basic and silicic magmas: a reflection of their source regions? *Contrib. Mineral. Petrol.* **106**, 129-141.

CONREY, R.M. (1990): Olivine analcimite in the Cascade Range of Oregon. *J. Geophys. Res.* **95**, 19639-19649.

_____, SHERROD, D.R. & HOOPER, P.R. (1994): Changes in basalt chemistry with intra-arc rifting, Cascade Range, Oregon and Washington, U.S.A. *Geol. Soc. Am., Abstr. Programs* **26**, A332.

_____, _____, UTO, K. & UCHIUMI, S. (1996a): Potassium–argon ages from Mount Hood area of Cascade Range, northern Oregon. *Isochron/West* **63**, 10-20.

_____, UTO, K., UCHIUMI, S., BEESON, M.H. MADIN, I.P., TOLAN, T.L. & SWANSON, D.A. (1996b): Potassium–argon ages of Boring Lava, northwest Oregon and southwest Washington. *Isochron/West* **63**, 3-9.

DEVEY, C.W., GARBE-SCHÖNBERG, C.-D., STOFFERS, P., CHAUVEL, C. & MERTZ, D.F. (1994): Geochemical effects of dynamic melting beneath ridges: reconciling major and trace element variations in Kolbeinsey (and global) mid-ocean ridge basalt. *J. Geophys. Res.* **99**, 9077-9095.

DICK, H.J.B. & BULLEN, T. (1984): Chromian spinel as a petrogenetic indicator in abyssal and alpine-type peridotites and spatially associated lavas. *Contrib. Mineral. Petrol.* **86**, 54-76.

DONALDSON, C.H. & BROWN, R.W. (1977): Refractory megacrysts and magnesium-rich melt inclusions within spinel in oceanic tholeiites: indicators of magma mixing and parental magma composition. *Earth Planet. Sci. Lett.* **37**, 81-89.

DONNELLY-NOLAN, J.M., CHAMPION, D.E., GROVE, T.L., BAKER, M.B., TAGGART, J.E., JR. & BRUGGMAN, P.E. (1991): The Giant Crater lava field: geology and geochemistry of a compositionally zoned, high-alumina basalt to basaltic andesite eruption at Medicine Lake volcano, California. *J. Geophys. Res.* **96**, 21,843-21,863.

DOWTY, E. (1980): Crystal growth and nucleation theory and the numerical simulation of igneous crystallization. *In* Physics of Magmatic Processes (R.B. Hargraves, ed.). Princeton University Press, Princeton, New Jersey (419-485).

EGGINS, S.M. (1992): Petrogenesis of Hawaiian tholeiites. 2. Aspects of dynamic melt segregation. *Contrib. Mineral. Petrol.* **110**, 398-410.

ELLIOTT, T.R., HAWKESWORTH, C.J. & GRÖNVOLD, K. (1991): Dynamic melting of the Iceland plume. *Nature* **351**, 201-206.

FALLOON, T.J., GREEN, D.H., HATTON, C.J. & HARRIS, K.L. (1988): Anhydrous partial melting of a fertile and depleted peridotite from 2 to 30 kb and application to basalt petrogenesis. *J. Petrol.* **29**, 1257-1282.

FISK, M.R. (1986): Basalt magma interaction with harzburgite and the formation of high-magnesium andesites. *Geophys. Res. Lett.* **13**, 467-470.

FOLEY, S. (1991): High-pressure stability of the fluor- and hydroxy-endmembers of pargasite and K-richterite. *Geochim. Cosmochim. Acta* **55**, 2689-2694.

FUKUYAMA, H. (1985): Heat of fusion of basaltic magma. *Earth Planet. Sci. Lett.* **73**, 407-414.

GAETANI, G.A. & GROVE, T.L. (1995): Estimating the pressure of melting for arc magmas: experimental determination of the partitioning of Fe and Mg among mantle minerals and hydrous primary magmas at 12 to 20 kbar. *Trans. Am. Geophys. Union (Eos)* **76**, F654 (abstr.).

_____, _____ & BRYAN, W.B. (1993): The influence of water on the petrogenesis of subduction-related igneous rocks. *Nature* **365**, 332-334.

GILL, J. & WHELAN, P. (1989): Early rifting of an oceanic arc (Fiji) produced shoshonitic to tholeiitic basalts. *J. Geophys. Res.* **94**, 4561-4578.

GREEN, T.H. & PEARSON, N.J. (1986): Ti-rich accessory phase saturation in hydrous mafic–felsic compositions at high P, T. *Chem. Geol.* **54**, 185-201.

GUFFANTI, M., CLYNNE, M.A., SMITH, J.G., MUFFLER, L.J.P. & BULLEN, T.D. (1990): Late Cenozoic volcanism, subduction, and extension in the Lassen region of California, southern Cascade Range. *J. Geophys. Res.* **95**, 19453-19464.

GUNN, S.H., CONREY, R.M. & SHERROD, D.R. (1996): Sr, Pb and Nd isotopic study of Cascade Range basalts in northern Oregon: constraints on mantle heterogeneity in a subduction zone. *Geol. Soc. Am., Abstr. Program* **28**, 71.

HART, W.K. (1985): Chemical and isotopic evidence for mixing between depleted and enriched mantle, northwestern U.S.A. *Geochim. Cosmochim. Acta* **49**, 131-144.

_____, ARONSON, J.L. & MERTZMAN, S.A. (1984): Areal distribution and age of low-K, high-alumina olivine tholeiite magmatism in the northwestern Great Basin. *Geol. Soc. Am., Bull.* **95**, 186-195.

HAWKESWORTH, C.J., ROGERS, N.W., VAN CALSTEREN, P.W.C. & MENZIES, M.A. (1984): Mantle enrichment processes. *Nature* **311**, 331-335.

HIROSE, K. & KUSHIRO, I. (1993): Partial melting of dry peridotites at high pressures: determination of compositions of melts segregated from peridotite using aggregates of diamond. *Earth Planet. Sci. Lett.* **114**, 477-489.

HOCHSTAEDTER, A.G., KEPEZHINSKAS, P., DEFANT, M., DRUMMOND, M. & KOLOSKOV, A. (1996): Insights into the volcanic arc mantle wedge from magnesian lavas from the Kamchatka arc. *J. Geophys. Res.* **101**, 697-712.

HOUSH, T.B. & LUHR, J.F. (1991): Plagioclase–melt equilibria in hydrous systems. *Am. Mineral.* **76**, 477-492.

HSUI, A.T. & TOKSÖZ, M.N. (1979): The evolution of thermal structures beneath a subduction zone. *Tectonophys.* **60**, 43-60.

HUGHES, S.S. (1990): Mafic magmatism and associated tectonism of the central High Cascade Range, Oregon. *J. Geophys. Res.* **95**, 19,623-19,638.

_____ & TAYLOR, E.M. (1986): Geochemistry, petrogenesis, and tectonic implications of central High Cascade mafic platform lavas. *Geol. Soc. Am., Bull.* **97**, 1024-1036.

IDDINGS, J.P. (1895): Absarokite – shoshonite – banakite series. *J. Geol.* **3**, 935-959.

JAQUES, A.L. & GREEN, D.H. (1980): Anhydrous melting of peridotite at 0–15 kb pressure and the genesis of tholeiitic basalts. *Contrib. Mineral. Petrol.* **73**, 287-310.

JUREWICZ, A.J.G. & WATSON, E.B. (1988): Cations in olivine. 1. Calcium partitioning and calcium–magnesium distribution between olivines and coexisting melts, with petrologic applications. *Contrib. Mineral. Petrol.* **99**, 176-185.

KAY, R.W. (1984): Elemental abundances relevant to identification of magma sources. *Phil. Trans. Roy. Soc. London* **310 A**, 535-547.

KELEMEN, P.B., JOHNSON, K.T.M., KINZLER, R.J. & IRVING, A.J. (1990): High-field-strength element depletions in arc basalts due to mantle–magma interaction. *Nature* **345**, 521-524.

_____, SHIMIZU, N. & DUNN, T. (1993): Relative depletion of niobium in some arc magmas and the continental crust: partitioning of K, Nb, La and Ce during melt/rock reaction in the upper mantle. *Earth Planet. Sci. Lett.* **120**, 111-134.

KINZLER, R.J. & GROVE, T.L. (1992): Primary magmas of mid-ocean ridge basalts. 1. Experiments and methods. *J. Geophys. Res.* **97**, 6885-6906.

_____ & _____ (1993): Corrections and further discussion of the primary magmas of mid-ocean ridge basalts, 1 and 2. *J. Geophys. Res.* **98**, 22,339-22,347.

KLEIN, E.M. & LANGMUIR, C.H. (1987): Global correlations of ocean ridge basalt chemistry with axial depth and crustal thickness. *J. Geophys. Res.* **92**, 8089-8115.

KRESS, V.C. & CARMICHAEL, I.S.E. (1991): The compressibility of silicate liquids containing Fe_2O_3 and the effect of composition, temperature, oxygen fugacity and pressure on their redox states. *Contrib. Mineral. Petrol.* **108**, 82-92.

LANGMUIR, C.H., KLEIN, E.M. & PLANK, T. (1992): Petrological systematics of mid-ocean ridge basalts: constraints on melt generation beneath mid-ocean ridges. *In* Mantle Flow and Melt Generation at Mid-Ocean Ridges (J.P. Morgan, D.K. Blackman & J.M. Sinton, eds.). *Am. Geophys. Union, Geophys. Monograph* **71**, 183-280.

LEEMAN, W.P., SMITH, D.R., HILDRETH, W., PALACZ, Z. & ROGERS, N. (1990): Compositional diversity of late Cenozoic basalts in a transect across the southern Washington Cascades: implications for subduction zone magmatism. *J. Geophys. Res.* **95**, 19561-19582.

LIN, P.-N., STERN, R.J. & BLOOMER, S.H. (1989): Shoshonitic volcanism in the northern Mariana arc. 2. Large-ion lithophile and rare earth element abundances: evidence for the source of incompatible element enrichments in intraoceanic arcs. *J. Geophys. Res.* **94**, 4497-4514.

LUHR, J.F. (1997): Extensional tectonics and the diverse primitive volcanic rocks in the Western Mexican Volcanic Belt. *Can. Mineral.* **35**, 473-500.

_____, ALLAN, J.F., CARMICHAEL, I.S.E., NELSON, S.A. & HASENAKA, T. (1989): Primitive calc-alkaline and alkaline rock types from the western Mexican Volcanic Belt. *J. Geophys. Res.* **94**, 4515-4530.

LUX, D.R. (1981): *Geochronology, Geochemistry, and Petrogenesis of Basaltic Rocks from the Western Cascades, Oregon.* Ph.D. thesis, Ohio State Univ., Columbus, Ohio.

_____ (1982): K–Ar and ^{40}Ar–^{39}Ar ages of mid-Tertiary rocks from the Western Cascade Range, Oregon. *Isochron/West* **33**, 27-32.

MATTIOLI, G.S., BAKER, M.B., RUTTER, M.J. & STOLPER, E.M. (1989): Upper mantle oxygen fugacity and its relationship to metasomatism. *J. Geol.* **97**, 521-536.

MCCULLOCH, M.T. & GAMBLE, J.A. (1991): Geochemical and geodynamical constraints on subduction zone magmatism. *Earth Planet. Sci. Lett.* **102**, 358-374.

MCINNES, B.I.A. & CAMERON, E.M. (1994): Carbonated, alkaline hybridizing melts from a sub-arc environment: mantle wedge samples from the Tabar – Lihir – Tanga – Feni arc, Papua New Guinea. *Earth Planet. Sci. Lett.* **122**, 125-141.

MCKENZIE, D. & BICKLE, M.J. (1988): The volume and composition of melt generated by extension of the lithosphere. *J. Petrol.* **29**, 625-679.

_____ & O'NIONS, R.K. (1991): Partial melt distributions from inversion of rare earth element concentrations. *J. Petrol.* **32**, 1021-1091.

MENZIES, M., ROGERS, N., TINDLE, A. & HAWKESWORTH, C. (1987): Metasomatic and enrichment processes in lithospheric peridotites, an effect of asthenosphere–lithosphere interaction. *In* Mantle Metasomatism (M.A. Menzies & C.J. Hawkesworth, eds.). Academic Press, London, U.K. (313-361).

MICHAEL, P.J. & CHASE, R.L. (1987): The influence of primary magma composition, H_2O and pressure on mid-ocean ridge basalt differentiation. *Contrib. Mineral. Petrol.* **96**, 245-263.

PANJASAWATWONG, Y., DANYUSHEVSKY, L.V., CRAWFORD, A.J. & HARRIS, K.L. (1995): An experimental study of the effects of melt composition on plagioclase–melt equilibria at 5 and 10 kbar: implications for the origin of magmatic high-An plagioclase. *Contrib. Mineral. Petrol.* **118**, 420-432.

PEARCE, J.A., BAKER, P.E., HARVEY, P.K. & LUFF, I.W. (1995): Geochemical evidence for subduction fluxes, mantle melting and fractional crystallization beneath the South Sandwich Island Arc. *J. Petrol.* **36**, 1073-1109.

_____ & PARKINSON, I.J. (1993): Trace element models for mantle melting: application to volcanic arc petrogenesis. *In* Magmatic Processes and Plate Tectonics (H.M. Prichard, T. Alabaster, N.B.W. Harris & C.R. Neary, eds.). *Geol. Soc., Spec. Publ.* **76**, 373-403.

PECCERILLO, A. & TAYLOR, S.R. (1976): Geochemistry of Eocene calc-alkaline volcanic rocks from the Kastamonu area, northern Turkey. *Contrib. Mineral. Petrol.* **58**, 63-81.

PECK, D.L., GRIGGS, A.B., SCHLICKER, H.G., WELLS, F.G. & DOLE, H.M. (1964): Geology of the central and northern parts of the Western Cascade Range in Oregon. *U.S. Geol. Surv., Prof. Pap.* **449**.

PHILLIPS, W.M., KOROSEC, M.A., SCHASSE, H.W., ANDERSON, J.L. & HAGEN, R.A. (1986): K–Ar ages of volcanic rocks in southwest Washington. *Isochron/West* **47**, 18-24.

PLANK, T. & LANGMUIR, C.H. (1993): Tracing trace elements from sediment input to volcanic output at subduction zones. *Nature* **362**, 739-743.

PRIEST, G.R. (1990): Volcanic and tectonic evolution of the Cascade Volcanic Arc, central Oregon. *J. Geophys. Res.* **95**, 19583-19599.

RIGHTER, K., CARMICHAEL, I.S.E., BECKER, T. A. & RENNE, P.R. (1995): Pliocene–Quaternary volcanism and faulting at the intersection of the Gulf of California and the Mexican Volcanic Belt. *Geol. Soc. Am., Bull.* **107**, 612-626.

RITCHIE, B. (1987): *Tholeiitic Lavas from the Western Cascade Range, Oregon.* M.S. thesis, Univ. of Oregon, Eugene, Oregon.

ROCK, N.M.S. (1984): Nature and origin of calc-alkaline lamprophyres: minettes, vogesites, kersantites and spessartites. *Trans. Roy. Soc. Edin., Earth Sci.* **74**, 193-227.

ROEDER, P.L. (1994): Chromite: from the fiery rain of chondrules to the Kilauea Iki lava lake. *Can. Mineral.* **32**, 729-746.

_____ & EMSLIE, R.F. (1970): Olivine–liquid equilibrium. *Contrib. Mineral. Petrol.* **29**, 275-289.

ROGERS, N.W. & SETTERFIELD, T.N. (1994): Potassium and incompatible-element enrichment in shoshonitic lavas from the Tavua volcano, Fiji. *Chem. Geol.* **118**, 43-62.

RYERSON, F.J. & WATSON, E.B. (1987): Rutile saturation in magmas: implications for Ti–Nb–Ta depletion in island-arc basalts. *Earth Planet. Sci. Lett.* **86**, 225-239.

SATO, H. (1977): Nickel content of basaltic magmas: identification of primary magmas and a measure of the degree of olivine fractionation. *Lithos* **10**, 113-120.

SCHNEIDER, M.E. & EGGLER, D.H. (1986): Fluids in equilibrium with peridotite minerals: implications for mantle metasomatism. *Geochim. Cosmochim. Acta* **50**, 711-724.

SEKINE, T. & WYLLIE, P.J. (1982): The system granite–peridotite–H_2O at 30 kbar, with applications to hybridization in subduction zone magmatism. *Contrib. Mineral. Petrol.* **81**, 190-202.

SHAW, D.M. (1970): Trace element fractionation during anatexis. *Geochim. Cosmochim. Acta* **34**, 237-243.

SHEN, Y. & FORSYTH, D.W. (1995): Geochemical constraints on initial and final depths of melting beneath mid-ocean ridges. *J. Geophys. Res.* **100**, 2211-2237.

SHERROD, D.R. & SMITH, J.G. (1990): Quaternary extrusion rates of the Cascade Range, northwestern United States and southern British Columbia. *J. Geophys. Res.* **95**, 19,465-19,474.

SIMKIN, T. & SMITH, J.V. (1970): Minor-element distribution in olivine. *J. Geol.* **78**, 304-325.

SISSON, T.W. & GROVE, T.L. (1993a): Experimental investigations of the role of H_2O in calc-alkaline differentiation and subduction zone magmatism. *Contrib. Mineral. Petrol.* **113**, 143-166.

_____ & _____ (1993b): Temperatures and H_2O contents of low-MgO high-alumina basalts. *Contrib. Mineral. Petrol.* **113**, 167-184.

_____ & LAYNE, G.D. (1993): H_2O in basalt and basaltic andesite glass inclusions from four subduction-related volcanoes. *Earth Planet. Sci. Lett.* **117**, 619-635.

SMITH, G.A. (1986): *Stratigraphy, Sedimentology, and Petrology of Neogene Rocks in the Deschutes Basin, Central Oregon: a Record of Continental Margin Volcanism and its Influence on Fluvial Sedimentation in an Arc-Adjacent Basin.* Ph.D. thesis, Oregon State Univ., Corvallis, Oregon.

_____, SNEE, L.W. & TAYLOR, E.M. (1987): Stratigraphic, sedimentologic, and petrologic record of late Miocene subsidence of the central Oregon High Cascades. *Geology* **15**, 389-392.

SNYDER, D.A. & CARMICHAEL, I.S.E. (1992): Olivine–liquid equilibria and the chemical activities of FeO, NiO, Fe_2O_3, and MgO in natural basic melts. *Geochim. Cosmochim. Acta* **56**, 303-318.

STOLPER, E. & NEWMAN, S. (1994): The role of water in the petrogenesis of Mariana trough magmas. *Earth Planet. Sci. Lett.* **121**, 293-325.

SUDO, A. & TATSUMI, Y. (1990): Phlogopite and K-amphibole in the upper mantle: implication for magma genesis in subduction zones. *Geophys. Res. Lett.* **17**, 29-32.

SWANSON, D.A. (1991): Geologic map of the Tower Rock quadrangle, southern Cascade Range, Washington. *U.S. Geol. Surv., Open-File Rep.* **91-314** (scale 1:24,000).

TAKAHASHI, E. (1978): Partitioning of Ni^{2+}, Co^{2+}, Fe^{2+}, Mn^{2+} and Mg^{2+} between olivine and silicate melts: compositional dependence of partition coefficient. *Geochim. Cosmochim. Acta* **42**, 1829-1844.

TATSUMI, Y. (1981): Melting experiments on a high-magnesian andesite. *Earth Planet. Sci. Lett.* **54**, 357-365.

_____ (1989): Migration of fluid phases and genesis of basalt magmas in subduction zones. *J. Geophys. Res.* **94**, 4697-4707.

_____ & KOYAGUCHI, T. (1989): An absarokite from a phlogopite lherzolite source. *Contrib. Mineral. Petrol.* **102**, 34-40.

_____ & MARUYAMA, S. (1989): Boninites and high-Mg andesites: tectonics and petrogenesis. *In* Boninites (A.J. Crawford, ed.). Unwin Hyman, London, U.K. (50-71).

THIBAULT, Y., EDGAR, A.D. & LLOYD, F.E. (1992): Experimental investigation of melts from a carbonated phlogopite lherzolite: implications for metasomatism in the continental lithospheric mantle. *Am. Mineral.* **77**, 784-794.

UMINO, S. & KUSHIRO, I. (1989): Experimental studies on boninite petrogenesis. *In* Boninites (A.J. Crawford, ed.). Unwin Hyman, London, U.K. (89-111).

VERPLANCK, E.P. (1985): *Temporal Variations in Volume and Geochemistry of Volcanism in the Western Cascades, Oregon.* M.S. thesis, Oregon State Univ., Corvallis, Oregon.

_____ & DUNCAN, R.A. (1987): Temporal variations in plate convergence and eruption rates in the Western Cascades, Oregon. *Tectonics* **6**, 197-209.

WELLS, R.E., ENGEBRETSON, D.C., P.D. SNAVELY, J. & COE, R.S. (1984): Cenozoic plate motions and the volcano-tectonic evolution of western Oregon and Washington. *Tectonics* **3**, 275-294.??

WENDLANDT, R.F. & EGGLER, D.H. (1980): The origins of potassic magmas. 2. Stability of phlogopite in natural spinel lherzolite and in the system $KAlSiO_4$–MgO–SiO_2–H_2O–CO_2 at high pressures and high temperatures. *Am. J. Sci.* **280**, 421-458.

WOOD, B.J., BRYNDZIA, L.T. & JOHNSON, K.E. (1990): Mantle oxidation state and its relationship to tectonic environment and fluid speciation. *Science* **248**, 337-345.

WOODHEAD, J., EGGINS, S. & GAMBLE, J. (1993): High field strength and transition element systematics in island arc and back-arc basin basalts: evidence for multi-phase melt extraction and a depleted mantle wedge. *Earth Planet. Sci. Lett.* **114**, 491-504.

YODER, H.S., JR. (1965): Diopside–anorthite–water at five and ten kilobars and its bearing on explosive volcanism. *Carnegie Inst. Wash. Yearbook* **64**, 82-89.

YOGODZINSKI, G.M., KAY, R.W., VOLYNETS, O.N., KOLOSKOV, A.V. & KAY, S.M. (1995): Magnesian andesite in the western Aleutian Komandorsky region: implications for slab melting and processes in the mantle wedge. *Geol. Soc. Am., Bull.* **107**, 505-519.

_____, VOLYNETS, O.N., KOLOSKOV, A.V., SELIVERSTOV, N.I. & MATVENKOV, V.V. (1994): Magnesian andesites and the subduction component in a strongly calc-alkaline series at Piip volcano, far western Aleutians. *J. Petrol.* **35**, 163-204.

Received February 6, 1996, revised manuscript accepted July 26, 1996.